

1 The Monash Simple Climate Model 2 Experiments (MSCM-DB v1.0): An 3 interactive database of mean climate, 4 climate change and scenario simulations

5 By Dietmar Dommenges^{1*}, Kerry Nice^{1,4}, Tobias Bayr², Dieter Kasang³, Christian
6 Stassen¹ and Mike Rezny¹

7

8 *: corresponding author; dietmar.dommenges@monash.edu

9 1: Monash University, School of Earth, Atmosphere and Environment, Clayton, Victoria
10 3800, Australia.

11 2: GEMOAR Helmholtz Centre for Ocean Research, Düsternbrooker Weg 20, 24105 Kiel,
12 Germany

13 3: DKRZ, Hamburg, Germany

14 4: Transport, Health, and Urban Design Hub, Faculty of Architecture, Building, and
15 Planning, University of Melbourne, Victoria 3010, Australia

16

17 submitted the Geoscientific Model Development, 8 March 2018

18 **Abstract**

19 This study introduces the Monash Simple Climate Model (MSCM) experiment
20 database. The simulations are based on the Globally Resolved Energy Balance
21 (GREB) model to study three different aspects of climate model simulations: (1)
22 understanding processes that control the mean climate, (2) the response of the
23 climate to a doubling of the CO₂ concentration, and (3) scenarios of external
24 forcing (CO₂ concentration and solar radiation). A series of sensitivity experiments
25 in which elements of the climate system are turned off in various combinations
26 are used to address (1) and (2). This database currently provides more than 1,300
27 experiments and has an online web interface for fast analysis and free access to
28 the data. We briefly outline the design of all experiments, give a discussion of some
29 results, put the findings into the context of previously published results from
30 similar experiments, discuss the quality and limitations of the MSCM experiments
31 and also give an outlook on possible further developments. The GREB model
32 simulation is quite realistic, but the model without flux corrections has a root
33 mean square error in the mean state of the surface temperature of about 10°C,
34 which is larger than those of general circulation models (2°C). It needs to be noted
35 here that the GREB model does not simulate circulation changes or changes in
36 cloud cover (feedbacks). However, the MSCM experiments show good agreement
37 to previously published studies. Although GREB is a very simple model, it delivers
38 good first-order estimates, is very fast, highly accessible, and can be used to
39 quickly try many different sensitivity experiments or scenarios. It builds a basis
40 on which conceptual ideas can be tested to a first-order and it provides a null
41 hypothesis for understanding complex climate interactions in the context of
42 response to external forcing or the interactions in the climate subsystems.

43 1. Introduction

44 Our understanding of the dynamics of the climate system and climate changes is
45 strongly linked to the analysis of model simulations of the climate system using a
46 range of climate models that vary in complexity and sophistication. Climate model
47 simulations help us to predict future climate changes and they help us to gain a
48 better understanding of the dynamics of this complex system.

49 State-of-the-art climate models, such as used in the Coupled Model Inter-
50 comparison Project (CMIP; Taylor et al. 2012), are highly complex simulations that
51 require significant amounts of computing resources and time. Such model
52 simulations require a significant amount of preparation. The development of
53 idealized experiments that would help in the understanding and modelling of
54 climate system processes are often difficult to realize with the complex CMIP-type
55 climate models. In this context, simplified climate models are useful, as they
56 provide a fast first guess that help to inform more complex models. They also help
57 in understanding the interactions in the complex system.

58 In this article, we introduce the Monash Simple Climate Model (MSCM) database
59 (version: MSCM-DB v1.0). The MSCM is an interactive website
60 (<http://mscm.dkrz.de>, Germany and <http://monash.edu/research/simple-climate-model>, Australia) and database that provides access to a series of more
61 than 1,300 experiments with the Globally Resolved Energy Balance (GREB) model
62 [Dommenget and Floter 2011; here after referred to as DF11]. The GREB model
63 was primarily developed to conceptually understand the physical processes that
64 control the global warming pattern in response to an increase in CO_2
65 concentration. It therefore centres around the surface temperature (T_{surf})
66 tendency equation, and only simulates the processes and variables needed for
67 resolving the global warming pattern.

68 Simplified climate models, such as Earth System Models of Intermediate
69 Complexity (EMICs), often aim at reducing the complexity to increase the
70 computation speed and therefore allow faster model simulations (e.g. CLIMBER
71 [Petoukhov et al. 2000], UVic [Weaver et al. 2001], FAMOUS [Smith et al. 2008] or
72 LOVECLIM [Goosse et al. 2010]). These EMICs are very similar in structure to
73 state-of-the-art Coupled General Circulation Models (CGCMs), following the
74 approach of simulating the geophysical fluid dynamics. The GREB model differs,
75 in that it follows an energy balance approach and does not simulate the
76 geophysical fluid dynamics of the atmosphere. It is therefore a climate model that
77 does not include weather dynamics, but focusses on the long term mean climate
78 and its response to external boundary changes. It further also does not include
79 cloud feedbacks or adjustments in the atmospheric circulation, as both are given
80 as boundary conditions. However, it does include the most important water vapor,
81 black-body radiation and ice-albedo feedbacks.

82 The purpose of the MSCM database for research studies are the following:

83

84

- 85 • **First Guess:** The MSCM provides first guesses for how the climate may
86 change in idealized or realistic experiments. The MSCM experiments can be
87 used to test ideas before implementing and testing them in more detailed
88 CGCM simulations.

- 89 • **Null Hypothesis:** The simplicity of the GREB model provides a good null
90 hypothesis for understanding the climate system. Because it does not
91 simulate weather dynamics or circulation changes of neither large nor

92 small scale it provides the null hypothesis of a climate as a pure energy
93 balance problem.

- 94 • **Conceptual understanding:** The simplicity of the GREB model helps to
95 better understand the interactions in the complex climate and, therefore,
96 helps to formulate simple conceptual models for climate interactions.
- 97 • **Education:** Studying the results of the MSCM helps to understand the
98 interactions that control the mean state climate and its regional and
99 seasonal differences. It helps to understand how the climate will respond
100 to external forcings in a first-order approximation.

101
102 The MSCM provides interfaces for fast analysis of the experiments and selection
103 of the data (see Figs. 1-3). It is designed for teaching and outreach purposes, but
104 also provides a useful tool for researchers. The focus in this study will be on
105 describing the research aspects of the MSCM, whereas the teaching aspects of it
106 will not be discussed. The MSCM experiments focus on three different aspects of
107 climate model simulations: (1) understanding the processes that control the mean
108 climate, (2) the response of the climate to a doubling of the CO_2 concentration, and
109 (3) scenarios of external CO_2 concentration and solar radiation forcings. We will
110 provide a short outline of the design of all experiments, give a brief discussion of
111 some results, and put the findings into context of previously published literature
112 results from similar experiments.

113 The DF11 study focussed primarily on the development of the model equations
114 and the discussion of the response pattern to an increase in CO_2 concentration.
115 This study here will give a more detailed discussion on the performance of the
116 GREB model on simulation of the mean state climate and on a wider range of
117 external forcing scenarios, including solar radiation changes.

118 The paper is organized as follows: The following section describes the GREB
119 model, the experiment designs, the MSCM interface, and the input data used. A
120 short analysis of the experiments is given in section 3. This section will mostly
121 focus on the GREB model performance in comparison to observations and
122 previously published simulations in the literature, but it will also give some
123 indications of the findings in the model experiments and the limitations of the
124 GREB model. The final section will give a short summary and outlook for potential
125 future developments and analysis.

126 **2. Model and experiment descriptions**

127 The GREB model is the underlying modelling tool for the MSCM interface. The
128 development of the model and all equations have been presented in DF11. The
129 model is simulating the global climate on a horizontal grid of 3.75° longitude x
130 3.75° latitude and in three vertical layers: surface, atmosphere and subsurface
131 ocean. It simulates four prognostic variables: surface, atmospheric and subsurface
132 ocean temperature, and atmospheric humidity (column integrated water vapor),
133 see appendix eqs. A1-4. It further simulates a number of diagnostic variables, such
134 as precipitation and snow/ice cover, resulting from the simulation of the
135 prognostic variables.

136 The main physical processes that control the surface temperature tendencies are
137 simulated: solar (short-wave) and thermal (long-wave) radiation, the hydrological
138 cycle (including evaporation, moisture transport and precipitation), horizontal

139 transport of heat and heat uptake in the subsurface ocean. Atmospheric
140 circulation and cloud cover are seasonally prescribed boundary condition, and
141 state-independent flux corrections are used to keep the GREB model close to the
142 observed mean climate. Thus, the GREB model does not simulate the atmospheric
143 or ocean circulation and is therefore conceptually very different from CGCM
144 simulations.

145 The model does simulate important climate feedbacks such as the water vapour
146 and ice-albedo feedback, but an important limitation of the GREB model is that the
147 response to external forcings or model parameter perturbations do not involve
148 circulation or cloud feedbacks [Bony et al. 2006; Boucher et al. 2013; Bony et al.
149 2015]. Circulation and cloud feedbacks do alter the climate response to external
150 forcings on regional and, to a lesser extent on the global scale. The experiments of
151 this database neglect any effects resulting from cloud or circulation feedbacks.
152 These experiments should therefore only be considered as first guess estimates.
153 In the context of some of the results discussed further below we will point out
154 some of the limitations of the GREB model approach.

155 Input climatologies (e.g. T_{surf} or atmospheric humidity) for the GREB model are
156 taken from the NCEP reanalysis data from 1950-2008 [Kalnay et al. 1996], cloud
157 cover climatology from the ISCCP project [Rossow and Schiffer 1991], ocean
158 mixed layer depth climatology from Lorbacher et al. [2006], and topographic data
159 was taken from ECHAM5 atmosphere model [Roeckner et al. 2003].

160 GREB does not have any internal (natural) variability since daily weather systems
161 are not simulated. Subsequently, the control climate or response to external
162 forcings can be estimated from one single year. The primary advantage of the
163 GREB model in the context of this study is its simplicity, speed, and low
164 computational cost. A one year GREB model simulation can be done on a standard
165 PC computer in about 1 s (about 100,000 simulated years per day). It can do
166 simulations of the global climate much faster than any state-of-the-art climate
167 model and is therefore a good first guess approach to test ideas before they are
168 applied to more complex CGCMs. A further advantage is the lag of internal
169 variability which allows the detection of a response to external forcing much more
170 easily.

171 **a. Experiments for the mean climate deconstruction**

172 The conceptual deconstruction of the GREB model to understand the interactions
173 in the climate system that lead to the mean climate characteristics is done by
174 defining 11 processes (switches; see Fig. 1). For each of these switches, a term in
175 the model equations is set to zero or altered if the switch is “OFF”. The processes
176 and how they affect the model equations are briefly listed below (with a short
177 summary in Table 1). The model equations relevant for the experiments in this
178 study are briefly restated in the appendix section A1 for the purpose of explaining
179 each experimental setup in the MSCM.

180
181

182 **Ice-albedo:** The surface albedo (α_{surf}) and the heat capacity over ocean points
183 (γ_{surf}) are influenced by snow and sea ice cover. In the GREB model these are a
184 direct function of T_{surf} . When the ice-albedo switch is OFF the surface albedo of all
185 points is constant (0.1) and, for ocean points, γ_{surf} follows the prescribed ocean
186 mixed layer depth independent of T_{surf} (i.e. no ice-covered ocean).

187

188 **Clouds:** The cloud cover, CLD , influences the amount of solar radiation reaching
189 the surface (α_{clouds} in eq. [A5]) and the emissivity of the atmospheric layer, ε_{atmos} ,
190 for thermal radiation (eq. [A8]). When the clouds switch is OFF, the cloud cover is
191 set to zero.

192

193 **Oceans:** The ocean in the GREB model simulates subsurface heat storage with the
194 surface mixed layer (~upper 50-100m). When the ocean switch is OFF, the F_{ocean}
195 term in eq. [A1] is set to zero, eq. [A3] is set to zero and the heat capacity of all
196 ocean points is set to that of land points.

197

198 **Atmosphere:** The atmosphere in the GREB model simulates a number of
199 processes: The hydrological cycle, horizontal transport of heat, thermal radiation,
200 and sensible heat exchange with the surface. When the atmosphere switch is OFF,
201 eq. [A2] and [A4] are set to zero, the heat flux terms, F_{sense} and F_{latent} in eq. [A1] are
202 set to zero and the downward atmospheric thermal radiation term in eq. [A6] is
203 set to zero.

204

205 **Diffusion of Heat:** The atmosphere transports heat by isotropic diffusion (4th
206 term in eq. [A2]). When this process is switched OFF, the term is set to zero.

207

208 **Advection of Heat:** The atmosphere transports heat by advection following the
209 mean wind field, \vec{u} (5th term in eq. [A2]). When this process is switched OFF, the
210 term is set to zero.

211

212 **CO₂:** The CO₂ concentration affects the emissivity of the atmosphere, ε_{atmos} (eq.
213 [A9]). When this process is switched OFF, the CO₂ concentration is set to zero.

214

215 **Hydrological cycle:** The hydrological cycle in the GREB model simulates the
216 evaporation, precipitation, and transport of atmospheric water vapour (eq. [A4]).
217 It further simulates latent heat cooling at the surface and heating in the
218 atmosphere. When the hydrological cycle is switched OFF, eq. [A4] is set to zero,
219 the heat flux term F_{latent} in eq. [A1] is set to zero, and $viwv_{atmos}$ in eq. [A9] is set to
220 zero. Subsequently, atmospheric humidity is zero.

221 It needs to be noted here, that the atmospheric emissivity in the log-function
222 parameterization of eq. [A9] can become negative, if the hydrological cycle, cloud
223 cover and CO₂ concentration are switched OFF (set to zero). This marks an
224 unphysical range of the GREB emissivity function and we will discuss the
225 limitations of the GREB model in these experiments in Section 3b.

226

227 **Diffusion of Water Vapour:** The atmosphere transports water vapour by
228 isotropic diffusion (3rd term in eq. [A4]). When this process is switched OFF, the
229 term is set to zero.

230

231 **Advection of Water Vapour:** The atmosphere transports water vapour by
232 advection following the mean wind field, \vec{u} (5th term in eq. [A2]). When this
233 process is switched OFF, the term is set to zero.

234

235 **Model Corrections:** The model correction terms in eqs. [A1, A3 and A4]
236 artificially force the mean T_{surf} , T_{ocean} , and q_{air} climate to be as observed. When
237 the model correction is switched OFF, the three terms are set to zero. This will
238 allow the GREB model to be studied without any artificial corrections and
239 therefore help to evaluate the GREB model equations' skill in simulating the
240 climate dynamics.

241 It should be noted here that the model correction terms in the GREB model have
242 been introduced to study the response to doubling of the CO_2 concentration for the
243 current climate, which is a relative small perturbation if compared against the
244 other perturbations considered above. They are meaningful for a small
245 perturbation in the climate system, but are less likely to be meaningful when large
246 perturbations to the climate system are done (e.g. cloud cover set to zero).

247
248 Each different combination of the above-mentioned process switches defines a
249 different experiment. However, not all combinations of switches are possible,
250 because some of the process switches are depending on each other (see Table 1
251 and Fig. 1). The total number of experiments possible with these process switches
252 is 656. For each experiment, the GREB model is run for 50 years, starting from the
253 original GREB model climatology and the final year is presented as the climatology
254 of this experiment in the MSCM database.

255 **b. Experiments for the $2xCO_2$ response deconstruction**

256 In a similar way, as described above for the mean climate, the climate response to
257 a doubling of the CO_2 concentration can be conceptually deconstructed with a set
258 of GREB model experiments. These experiments help to understand the
259 interactions in the climate system that lead to the climate response to a doubling
260 of the CO_2 concentration. However, there are a number of differences that need to
261 be considered.

262 A meaningful deconstruction of the response to a doubling of the CO_2
263 concentration should consider the reference control mean climate since the
264 forcings and the feedbacks controlling the response are mean state dependent. We
265 therefore ensure that all sensitivity experiments in this discussion have the same
266 reference mean control climate. This is achieved by estimating the flux correction
267 term in eqs. [A1, A3 and A4] for each sensitivity experiment to maintain the
268 observed control climate. Thus, when a process is switched OFF, the control
269 climatological tendencies in eqs. [A1, S3 and S4] are the same as in the original
270 GREB model, but changes in the tendencies due to external forcings, such as
271 doubling of the CO_2 concentration are not affected by the disabled process. This is
272 the same approach as in DF11.

273 For the $2xCO_2$ response deconstruction experiments, we define 10 boundary
274 conditions or processes (switches; see Fig. 2). The Ice-albedo, advection and
275 diffusion of heat and water vapour, and the hydrological cycle processes are
276 defined in the same way as for the mean climate deconstruction (section 2a). The
277 remaining boundary conditions and processes are briefly listed below (and a short
278 summary is given in Table 2).

279

280 The following boundary conditions are considered:

281

282 **Topography:** The topography in the GREB model affects the amount of
283 atmosphere above the surface and therefore affects the emissivity of the
284 atmosphere in the thermal radiation (eq. [A9]). Regions with high topography
285 have less greenhouse gas concentrations in the thermal radiation (eq. [A9]). It
286 further affects the diffusion coefficient (κ) for transport of heat and moisture (eq.
287 [A2 and A4]). When the topography is turned OFF, all points of the GREB model
288 are set to sea level height and have the same amount of CO_2 concentration in the
289 thermal radiation (eq. [A9]).

290

291 **Clouds:** The cloud cover in the GREB model affects the incoming solar radiation
292 and the emissivity of the atmosphere in the thermal radiation (eq. [A9]). In
293 particular, it influences the sensitivity of the emissivity to changes in the CO_2
294 concentration. A clear sky atmosphere is more sensitive to changes in the CO_2
295 concentration than a fully cloud-covered atmosphere. When the cloud cover
296 switch is OFF, the observed cloud cover climatology boundary conditions are
297 replaced with a constant global mean cloud cover of 0.7. It is not set to zero to
298 avoid an impact on the global climate sensitivity, and to focus on the regional
299 effects of inhomogeneous cloud cover.

300

301 **Humidity:** Similarly, to the cloud cover, the amount of atmospheric water vapour
302 affects the emissivity of the atmosphere in the thermal radiation and, in particular,
303 the sensitivity to changes in the CO_2 concentration (eq. [A9]). A humid atmosphere
304 is less sensitive to changes in the CO_2 concentration than a dry atmosphere. When
305 the humidity switch is OFF, the constraint to the observed humidity climatology
306 (flux correction in eq. [A4]) is replaced with a constant global mean humidity of
307 0.0052 [kg/kg]. It is again not set to zero to avoid an impact on the global climate
308 sensitivity, but to focus on the regional effects of inhomogeneous humidity.

309

310 The additional feedbacks and processes considered are:

311

312 **Ocean heat uptake:** The ocean heat uptake in GREB is done in two ocean layers.
313 The largest part of the ocean heat is in the subsurface layer, T_{ocean} (eq. [A3]). When
314 the ocean switch is OFF the F_{ocean} term in eq. [A1] is set to zero, equation [A3] is
315 set to zero and the heat capacity (γ_{surf}) off all ocean points in eq. [A1] is set to that
316 of a 50m water column.

317

318 The total number of experiments with these process switches is 640. For each
319 experiment, the GREB model is run for 50 years, starting from the original GREB
320 model climatology, and doubling of the CO_2 concentrations in the first time-step.
321 The changes over the 50yrs period relative to the original GREB model climatology
322 of these experiments are presented in the MSCM database.

323 c. Scenario experiments

324 A number of different scenarios of external boundary condition changes exist in
325 the MSCM experiment database. They include different changes in the CO_2
326 concentration and in the incoming solar radiation. A complete overview is given
327 in Table 3. A short description follows below.

328

329 RCP-scenarios

330 In the Representative Concentration Pathways (RCP) scenarios the GREB model is
331 forced with time varying CO_2 concentrations. All five different simulations have
332 the same historical time evolution of CO_2 concentrations starting from 1850 to
333 2000, and from 2001 follow the RCP8.5, RCP6, RCP4.5, RCP2.6 and the A1B CO_2
334 concentration pathways until 2100 [van Vuuren et al. 2011].
335

336 **Idealized CO_2 scenarios**

337 The 15 idealized CO_2 concentration scenarios in the MSCM experiment database
338 focus on the non-linear time delay and regional differences in the climate response
339 to different CO_2 concentrations. These were implemented in five simulations in
340 which the control CO_2 concentration (340ppm) was changed in the first time step
341 to a scaled CO_2 concentration of 0, 0.5, 2, 4, and 10 times the control level. The
342 $0.5 \times CO_2$ and $2 \times CO_2$ simulations are 50yrs long and the others are 100yrs long.

343 Two different simulations with idealized time evolutions of CO_2 concentrations are
344 conducted to study the time delay of the climate response. In one simulation, the
345 CO_2 concentration is doubled in the first time-step, held at this level for 30yrs then
346 returned to control levels instantaneously ($2 \times CO_2$ abrupt reverse). In the second
347 simulation, the CO_2 concentration is varied between the control and $2 \times CO_2$
348 concentrations following a sine function with a period of 30yrs, starting at the
349 minimum of the sine function at the control CO_2 concentration ($2 \times CO_2$ wave). Both
350 simulations are 100yrs long.

351 The third set of idealized CO_2 concentration scenarios double the CO_2
352 concentrations restricted to different regions or seasons. The eight regions and
353 seasons include: the Northern or Southern Hemisphere, tropics ($30^\circ S$ - $30^\circ N$) or
354 extra-tropics (poleward of 30°), land or oceans and in the month October to March
355 or in the month April to September. Each experiment is 50yrs long.
356

357 **Solar radiation**

358 Two different experiments with changes in the solar constant were created. In the
359 first experiment, the solar constant is increased by about 2% ($+27W/m^2$), which
360 leads to about the same global warming as a doubling of the CO_2 concentration
361 [Hansen et al. 1997]. In the second experiment, the solar constant oscillates at an
362 amplitude of $1W/m^2$ and a period of 11yrs, representing an idealized variation of
363 the incoming solar short wave radiation due to the natural 11yr solar cycle
364 [Willson and Hudson 1991]. Both experiments are 50yrs long.
365

366 **Idealized orbital parameters**

367 A series of five simulations are done in the context of orbital forcings and the
368 related ice age cycles. In one simulation, the incoming solar radiation as function
369 of latitude and day of the year was changed to its values as it was 231Kyr ago
370 [Berger and Loutre 1991 and Huybers 2006]. In an additional simulation, the CO_2
371 concentration is reduced from 340ppm to 200ppm as observed during the peak of
372 ice age phases in combination with the incoming solar radiation changes. Both
373 simulations are 100yrs long.

374 In three sensitivity experiments, we changed the incoming solar radiation
375 according to some idealized orbital parameter changes to study the effect of the
376 most important orbital parameters. The orbital parameters changed are: the
377 distance to the sun, the Earth axis tilt relative to the Earth-Sun plane (obliquity)
378 and the eccentricity of the Earth orbit around the sun. The orbit radius was

379 changed from 0.8AU to 1.2AU in steps of 0.01AU, the obliquity from -25° to 90° in
380 steps of 2.5° and the eccentricity from 0.3 (Earth closest to the sun in July) to 0.3
381 (Earth furthest from the sun in July) in steps of 0.01. Each sensitivity experiment
382 was started from the control GREB model (1AU radius, 23.5° obliquity and 0.017
383 eccentricity) and run for 50yrs. The last year of each simulation is presented as
384 the estimate for the equilibrium climate.

385 **3. Some results of the model simulations**

386 The MSCM experiment database includes a large set of experiments that address
387 many different aspects of the climate. At the same time, the GREB model has
388 limited complexity and not all aspects of the climate system are simulated in the
389 GREB experiments. The following analysis will give a short overview of some of
390 the results that can be taken from the MSCM experiments. In this we will focus on
391 aspects of general interest and on comparing the outcome to results of other
392 published studies to illustrate the strength and limitations of the GREB model in
393 this context. The discussion, however, will be incomplete, as there are simply too
394 many aspects that could be discussed in this set of experiments. We will therefore
395 focus on a general introduction and leave space for future studies to address other
396 aspects.

397 **a. GREB model performance**

398 The skill of the GREB model is illustrated in Figure 4, by running the GREB model
399 without the correction terms. For reference, we compare this GREB run with the
400 observed mean climate and seasonal cycle (this is identical to running the GREB
401 model with correction terms) and with a bare world. The latter is the GREB model
402 with all switches OFF (radiative balance without an atmosphere and a dark
403 surface). In comparison with the full GREB model, this illustrates how much all the
404 climate processes affect the climate.

405 The GREB model without correction terms does capture the main features of the
406 zonal mean climate, the seasonal cycle, the land-sea contrast and even smaller
407 scale structures within continents or ocean basins (e.g. seasonal cycle structure
408 within Asia or zonal temperature gradients within ocean basins). For most of the
409 globe ($<50^\circ$ from the equator), the GREB model root-mean-squared error (RMSE)
410 for the annual mean T_{surf} is less than 10°C relative to the observed (see Fig. 4g).
411 This is larger than for state-of-the-art CMIP-type climate models, which typically
412 have an RMSE of about 2°C [Dommenget 2012]. In particular, the regions near the
413 poles have high RMSE. It seems likely that the meridional heat transport is the
414 main limitation in the GREB model, given the too warm tropical regions and the,
415 in general, too cold polar regions and the too strong seasonal cycle in the polar
416 regions in the GREB model without correction terms.

417 The GREB model performance can be put in perspective by illustrating how much
418 the climate processes simulated in the GREB model contribute to the mean climate
419 relative to the bare world simulation (see Fig. 4). The GREB RMSE to observed is
420 about 20-30% of the RMSE of the bare world simulation (not shown), suggesting
421 that the GREB model has a relative error of about 20-30% in the processes that it
422 simulates or due to processes that it does not simulate (e.g. ocean heat transport).

423 **b. Mean climate deconstruction**

424 Understanding what is causing the mean observed climate with its regional and
425 seasonal difference is often central for understanding climate variability and
426 change. For instance, the seasonal cycle is often considered as a first guess
427 estimate for climate sensitivity [Knutti et al. 2006]. In the following analysis, we
428 will give a short overview on how the 10 processes of the MSCM experiments
429 contribute to the mean climate and its seasonal cycle. For these experiments, we
430 use the GREB model without flux correction terms.

431 In the discussion of the experiments, it is important to consider that climate
432 feedbacks are contributing to the interactions of the climate processes. The effect
433 of a climate process on the climate is a result of all the other active climate
434 processes responding to the changes that the climate process under consideration
435 introduces. It also depends on the mean background climate. Therefore, it does
436 matter in which combination of switches the GREB model experiments are
437 discussed. For instance, the effect of the Ice/Snow cover, is stronger in a much
438 colder background climate, but is also affected by the feedback in other climate
439 processes, such as the water vapour feedback. We will therefore consider different
440 experiments or different experiment sets to shade some light into these
441 interactions.

442 In Figures 5 and 6 the contribution of each of the 10 processes (except the
443 atmosphere) to the annual mean climate (Fig. 5) and its seasonal cycle (Fig. 6) are
444 shown. In each experiment, all processes are active, but the process of interest and
445 the model correction terms are turned OFF. The results are compared against the
446 complete GREB model without the model correction terms (all processes active;
447 expect model correction terms). For the hydrological we will discuss some
448 additional experiments in which the ice-albedo feedback is turned OFF as well.

449 The Ice/Snow cover (Fig. 5a) has a strong cooling effect mostly at the high
450 latitudes in the cold season, which is due to the ice-albedo feedback. However, in
451 the warm season (not shown) the insulation effect of the sea ice actually leads to
452 warming, as the ocean cannot cool down as much during winter as it does without
453 sea ice.

454 The cloud cover in the GREB model is only considered as a given boundary
455 condition, but does not simulate the formation of clouds. Therefore, it does not
456 include cloud feedbacks. However, the mean cloud cover does influence the
457 radiation balance of solar and thermal radiation, and therefore affects the mean
458 climate and its seasonal cycle. Fig. 5b illustrates that cloud cover has a large net
459 cooling effect globally due to the solar radiation reflection effect dominating over
460 the thermal radiation warming effect. Previous studies on the cloud cover effect
461 on the overall climate mostly focus on the radiative forcings estimates, but to our
462 best knowledge, do not discuss by how much the mean surface temperature is
463 affected by the mean cloud cover [e.g. Rossow and Zhang 1995].

464 It is interesting to note that the strongest cooling effect of cloud cover is over
465 regions with fairly little cloud cover (e.g. deserts and mountain regions). Here it is
466 important to point out that the climate system response to any external forcing or
467 changes in the boundary conditions, such as CO₂-forcing or removing the cloud
468 cover, is dominated by internal positive feedback rather than the direct local
469 forcing effect (e.g. see discussion of the global warming pattern in DF11).

470 The most important internal positive feedback is the water vapor feedback, which
471 amplifies the effect of removing the cloud cover. This feedback is stronger over

472 dry and cold regions (DF11) and therefore amplifies the effects of removing the
473 cloud cover over deserts and mountain regions.

474 The large ocean heat capacity slows down the seasonal cycle (Fig. 6c).
475 Subsequently, the seasons are more moderate than they would be without the
476 ocean transferring heat from warm to cold seasons. This is, in particular,
477 important in the mid and higher latitudes. The effect of the ocean heat capacity,
478 however, has also an annual mean warming effect (Fig. 5c). This is due to the non-
479 linear thermal radiation cooling. The non-linear black body negative radiation
480 feedback is stronger for warmer temperatures, which are not reached in a
481 moderated seasonal cycle with the larger ocean heat capacity. Studies with more
482 complex climate models do find similar impacts of the ocean heat capacity on the
483 annual mean and on the seasonal cycle (e.g. Donohoe et al. 2014).

484 The diffusion of heat reduces temperature extremes (Fig. 5d). It therefore warms
485 extremely cold regions (e.g. polar regions) and cools the hottest regions (e.g. warm
486 deserts). In global averages, this is mostly cancelled out. The advection of heat has
487 strong effects where the mean winds blow across strong temperature gradients.
488 This is mostly present in the Northern Hemisphere (Fig. 5e). The most prominent
489 feature is the strong warming of the northern European and Asian continents in
490 the cold season. In global average, warming and cooling mostly cancel each other
491 out.

492 Literature discussions of heat transport are usually based on heat budget analysis
493 of the climate system (in observations or simulations) instead of 'switching off' the
494 heat transport in fully complex climate models, since such experiments are
495 difficult to conduct. A similar heat budget analysis of the GREB model experiments
496 is beyond the scope of this study, but the results in these experiments appear to
497 be largely consistent with the findings in heat budget analysis. For instance, the
498 regional contributions of diffusion and advection are similar to those found in
499 previous studies (e.g. Peixoto 1992; Yang et al. 2015).

500 The CO_2 concentration leads to a global mean warming of about 9 degrees (Fig.
501 5f). Even though it is the same CO_2 concentration everywhere, the warming effect
502 is different at different locations. This is discussed in more detail in DF11 and in
503 section 3c.

504 The input of water vapour into the atmosphere by the hydrological cycle leads to
505 a substantial amount of warming globally (Fig. 5g). However, we need to consider
506 that the experiment with switching OFF the hydrological cycle is the only
507 experiment in which we have a significant amount of global cooling (by about -
508 $44^\circ C$). As a result, most of the earth is below freezing temperatures and therefore
509 has a much stronger ice-albedo feedback than in any other experiment. This leads
510 to a significant amplification of the response.

511 It is instructive to repeat the experiments with the ice-albedo feedback switched
512 OFF (see supplementary Fig. 1). In these experiments, all processes show a
513 reduced impact on the annual mean temperatures, but the hydrological cycle is
514 most strongly affected by it. The ice-albedo effect almost doubles the hydrological
515 cycle response, while for all other processes the effect is about a 10% to 40%
516 increase. In the following discussions, we will therefore consider the hydrological
517 cycle impact with and without ice-albedo feedback. In the average of both
518 response (Fig. 5g and SFig. 1g) the hydrological cycle has a global mean impact of
519 about $+34^\circ C$ with strongest amplitudes in the tropics. It is still the strongest of all
520 processes.

521 Similar to the oceans, the hydrological cycle dampens the seasonal cycle (Fig. 6g),
522 but with a much weaker amplitude. The transport of water vapour away from
523 warm and moist regions (e.g. tropical oceans) to cold and dry regions (e.g. high
524 latitudes and continents) leads to additional warming in the regions that gain
525 water vapour and cooling to those that lose water vapour (Fig. 6h). The effect is
526 similar in both hemispheres. The transport of water vapour along the mean wind
527 directions has stronger effects on the Northern Hemisphere than on the Southern
528 Hemisphere, since the northern hemispheric mean winds have more of a
529 meridional component, which creates advection across water vapour gradients
530 (Fig. 6i). This effect is most pronounced in the cold seasons.

531 Most processes have a predominately zonal structure. We can therefore take a
532 closer look at the zonal mean climate and seasonal cycle of all processes to get a
533 good representation of the relative importance of each process, see Fig. 7. The
534 annual mean climate is most strongly influenced by the hydrological cycle (here
535 shown as the mean of the response with and without the ice-albedo feedback). The
536 cloud cover has an opposing cooling effect, but is weaker than the warming effect
537 of the hydrological cycle. The warming effect by the ocean's heat capacity is similar
538 in scale to that of the CO_2 concentration.

539 An interesting aspect of the climate system is that the Northern hemisphere is
540 warmer than the Southern counterpart (by about $1.5^\circ C$; not shown), which may
541 be counterintuitive given the warming effect of the ocean heat capacity (see above
542 discussion; Kang et al. 2015). The GREB model without flux correction also does
543 have a warmer Northern hemisphere than the Southern counterpart (by about
544 $0.3^\circ C$; not shown), whereas the bare earth (pure blackbody radiation balance;
545 GREB all switches OFF) would have the Northern hemisphere colder than the
546 Southern counterpart (by about $-0.6^\circ C$; not shown). A number of processes play
547 into this inter-hemispheric contrast, with the most important contribution coming
548 from the cross-equatorial heat and moisture advection (see Fig. 7a). This is largely
549 consistent with Kang et al. (2015).

550 The seasonal cycle is damped most strongly by the ocean's heat capacity and by
551 the hydrological cycle. The latter may seem unexpected, but is due to the effect
552 that the increased water vapour has a stronger warming effect in the cold seasons,
553 similarly to the greenhouse effect of CO_2 concentrations. In turn, the ice/snow
554 cover and cloud cover lead to an intensification of the seasonal cycle at higher
555 latitudes. Again, the latter may seem unexpected, but is due to the interaction with
556 other climate feedbacks such as the water vapour feedback, which also makes the
557 climate more strongly respond to changes in cloud cover in regions where there
558 actually is very little cloud cover (e.g. deserts).

559 As an alternative way of understanding the role of the different process we can
560 build up the complete climate by introducing one process after the other, see Figs.
561 8 and 9. We start with the bare earth (e.g. like our Moon) and then introduce one
562 process after the other. The order in which the processes are introduced is mostly
563 motivated by giving a good representation for each of the 10 processes. However,
564 it can also be interpreted as a build up the Earth climate in a somewhat historical
565 way: We assume that initially the earth was a bare planet and then the
566 atmosphere, ocean, and all the other aspects were build up over time.

567 The Bare Earth (all switches OFF) is a planet without atmosphere, ocean or ice. It
568 has an extremely strong seasonal cycle (Fig. 9a) and is much colder than our
569 current climate (Fig. 8a). It also has no regional structure other than meridional

570 temperature gradients. The combination of all climate processes will create most
571 of the regional and seasonal difference that make our current climate.

572 The atmospheric layer in the GREB model simulates two processes, if all other
573 processes are turned off: a turbulent sensible heat exchange with the surface and
574 thermal radiation due to residual trace gasses other than CO_2 , water vapour or
575 clouds. However, as mentioned in the appendix A1 the log-function approximation
576 leads to negative emissivity if all greenhouse gasses (CO_2 and water vapour)
577 concentrations and cloud cover are zero. The negative emissivity turns the
578 atmospheric layer into a cooling effect, which dominates the impact of the
579 atmosphere in this experiment (Figs. 8b, c). This is a limitation of the GREB model
580 and the result of this experiment as such should be considered with caution. In a
581 more realistic experiment we can set the emissivity of the atmosphere to zero or
582 a very small value (0.01) to simulate the effect of the atmosphere without CO_2 ,
583 water vapour and cloud cover, see SFig. 2. Both experiments have very similar
584 warming effects in polar regions. Suggesting that the sensible heat exchange
585 warms the surface. The residual thermal radiation effect from the emissivity of
586 0.01 has only a minor impact (SFig. 2f and g).

587 The warming effect of the CO_2 concentration is nearly uniform (Figs. 8d, e) and
588 without much of a seasonal cycle (Figs. 9d, e), if all other processes are turned OFF.
589 This accounts for a warming of about $+9^\circ C$.

590 The large ocean heat capacity reduces the amplitude of the seasonal cycle (Figs.
591 9f, g). The effective heat capacity of the oceans is proportional to the observed
592 mixed layer in the GREB model, which causes some small variations (differences
593 from the zonal means) as seen in the seasonal cycle of the oceans. Land points are
594 not affected, since no atmospheric transport exist (advection and diffusion turned
595 OFF). The different heat capacity between oceans and land already make a
596 significant element of the regional and seasonal climate differences (Figs. 8f, g).

597 Introducing turbulent diffusion of heat in the atmosphere now enables interaction
598 between points, which has the strongest effects along coastlines and in higher
599 latitudes (Figs. 8h, i). It reduces the land-sea contrast and has strong effects over
600 land with warming in winter and cooling in summer (Figs. 9h, i). The extreme
601 climates of the winter polar region are most strongly affected by the turbulent
602 heat exchange with lower latitudes. The turbulent heat exchange makes the
603 regional climate difference again a bit more realistic.

604 The advection of heat is strongly dependent on the temperature gradients along
605 the mean wind field directions. It provides substantial heating during the winter
606 season for Europe, Russia, and western North America (Figs. 8j, k, 9j, k). The
607 structure (differences from the zonal mean) created by this process is mostly
608 caused by the prescribed mean wind climatology. In particular, the milder climate
609 in Europe compared to northeast Asia on the same latitudes, are created by wind
610 blowing from the ocean onto land. The same is true for the differences between
611 the west and east coasts of northern North America. The climate regional and
612 seasonal structures are now already quite realistic, but the overall climate is much
613 too cold. The ice/snow cover further cools the climate, in particular, the polar
614 regions (Figs. 8l, m). This difference illustrates that the ice-albedo feedback is
615 primarily leading to cooling in higher latitudes and mostly in the winter season.

616 Introducing the hydrological cycle brings the most important greenhouse gas into
617 the atmosphere: water vapour. This has an enormous warming effect globally
618 (Figs. 8n, o) and a moderate reduction in the strength of the seasonal cycle (Figs.

619 9n, o). The resulting modelled climate is now much too warm, but introducing the
620 cloud cover cools the climate substantially (Figs. 8p, q) and leads to a fairly
621 realistic climate.

622 The atmospheric transport (diffusion and advection) brings water vapour from
623 relative moist regions to relatively dry regions (Figs. 8r, s). This leads to enhanced
624 warming in the dry and cold regions (e.g. Sahara Desert or polar regions) by the
625 water vapour thermal radiation (greenhouse) effect and cooling in the regions
626 where it came from (e.g. tropical oceans). The heating effect is similar to the
627 transport of heat and has also a strong seasonal cycle component.

628 In the above discussion on how the individual climate processes affect the climate
629 we have to keep in mind the limitations of the GREB model and the experimental
630 setups. The climate response to changing a single climate element is more complex
631 in the real world than simulated in these GREB experiments. For instance, if the
632 ocean heat capacity is turned 'OFF' it will not just have an effect on the effective
633 heat capacity, but the resulting changes in surface temperature gradients will also
634 affect the atmospheric circulation patterns and subsequently the cloud cover. Such
635 effects on the atmospheric circulation and cloud cover are neglected in the GREB
636 model, as they are given as fixed boundary conditions. Regionally such effects can
637 be significant and CGCM simulations are required to study such effects.

638 **c. $2xCO_2$ response deconstruction**

639 The doubling of the CO_2 concentrations leads to a distinct warming pattern with
640 polar amplification, a land-sea contrast and significant seasonal differences in the
641 warming rate. These structures in the warming pattern reflect the complex
642 interactions between feedbacks in the climate system and regional difference in
643 CO_2 forcing pattern. The MSCM $2xCO_2$ response experiments are designed to help
644 understand the interactions causing this distinct warming pattern. DF11
645 discussed many aspects of these experiments with focus on the land-sea contrast,
646 the seasonal differences, and the polar amplification. We therefore will focus here
647 only on some aspects that have not been previously discussed in DF11.

648 In the GREB model, we can turn OFF the atmospheric transport and therefore
649 study the local interaction without any lateral interactions. Figure 10 shows three
650 experiments in which the atmospheric transport and other processes (see Figure
651 caption) are inactive. The three experiments highlight the regional difference in
652 the CO_2 forcing pattern and in the two main feedbacks (water vapour and ice-
653 albedo).

654 In the first experiment (Fig. 10a) without feedback processes, the local T_{surf}
655 response is approximately directly proportional to the local CO_2 forcing. The
656 regional differences are caused by differences in the cloud cover and atmospheric
657 humidity, since both influence the thermal radiation effect of CO_2 [DF11, Kiehl and
658 Ramanathan 1982 and Cess et al. 1993]. This causes, on average, the land regions
659 to see a stronger forcing than oceanic regions (see Fig. 10b). However, even over
660 oceans we can see clear differences. For instance, the warm pool of the western
661 tropical Pacific sees less CO_2 forcing than the eastern tropical Pacific.

662 The ice-albedo feedback is strongly localized and it is strongest over the mid-
663 latitudes of the northern continents and at the sea ice edge of around Antarctica
664 (Figs. 10c and d). The water vapour feedback is far more wide-spread and stronger
665 (Figs. 10e and f). It is strongest in relatively warm and dry regions (e.g. subtropical

666 oceans), but also shows some clear localized features, such as the strong Arabian
667 or Mediterranean Seas warming.

668 **d. Scenarios**

669 The set of scenario experiments in the MSCM simulations allows us to study the
670 response of the climate system to changes in the external boundary conditions in
671 a number of different ways. In the following, we will briefly illustrate some results
672 from these scenarios and organize the discussion by the different themes in
673 scenario experiments.

674 The CMIP project has defined a number of standard CO_2 concentration projection
675 simulations, that give different RCP scenarios for the future climate change, see
676 Fig. 11a. The GREB model sensitivity in these scenarios is similar to those of the
677 CMIP database [Forster et al. 2013].

678 Idealized CO_2 concentration scenarios help to understand the response to the CO_2
679 forcing. In Figure 11b, we show the global mean T_{surf} response to different scaling
680 factors of CO_2 concentrations. To first order, we can see that the global mean T_{surf}
681 response follows a logarithmic CO_2 concentration (e.g. any doubling of the CO_2
682 concentration leads to the same global mean T_{surf} response; compare $2xCO_2$ with
683 $4xCO_2$ or with in Fig.11b) as suggested in other studies [Myhre et al. 1998].
684 However, this relationship does breakdown if we go to very low CO_2
685 concentrations (e.g. zero CO_2 concentration) illustrating that the log-function
686 approximation of the CO_2 forcing effect is only valid within a narrow range far
687 away from zero CO_2 concentration.

688 The transient response time to CO_2 forcing can be estimated from idealized CO_2
689 concentration changes, see Fig. 11c. The step-wise change in CO_2 concentration
690 illustrates the response time of the global climate. In the GREB model, it takes
691 about 10yrs to get 80% of the response to a CO_2 concentration change (see step-
692 function response, Fig. 11c). In turn, the response to a CO_2 concentration wave
693 time evolution is a lag of about 3yrs. The fast versus slow response also leads to
694 different warming patterns with strong land-sea contrasts (not shown), that are
695 largely similar to those found in previous studies [Held et al. 2010].

696 The regional aspects of the response to a CO_2 concentration can also be studied by
697 partially increasing the CO_2 concentration in different regions, see Fig. 12. The
698 warming response mostly follows the regions where we partially changed the CO_2
699 concentration, but there are some interesting variations in this. The partial
700 increase in the CO_2 concentration over oceans has a stronger warming impact than
701 the partial increase in the CO_2 concentration over land for most Southern
702 Hemisphere land regions. In turn, the land forcing has little impact for the ocean
703 regions. The boreal winter forcing has stronger impact on the Southern
704 Hemisphere than boreal summer forcing, suggesting that the warm season forcing
705 is, in general, more important than the cold season forcing. The only exception to
706 this is the Tibet-plateau region.

707 A series of scenarios focus on the impact of solar forcing. In Figure 11d, we show
708 the response to an idealized 11yr solar cycle. The global mean T_{surf} response is two
709 orders of magnitude smaller than the response to a doubling of the CO_2
710 concentration, reflecting the weak amplitude of this forcing. This result is largely
711 consistent with the response found in GCM simulations [Cubasch et al. 1997], but
712 does not consider possible more complicated amplification mechanisms [Meehl et
713 al. 2009]. A change in the solar constant of $+27W/m^2$ has a global T_{surf} warming

714 response similar to a doubling of the CO_2 concentration, but with a slightly
715 different warming pattern, see Fig. 13. The warming pattern of a solar constant
716 change has a stronger warming where incoming sun light is stronger (e.g. tropics
717 or summer season) and a weaker warming in region with less incoming sun light
718 (e.g. higher latitudes or winter season). This is in general agreement with other
719 modelling studies [Hansen et al. 1997].

720 On longer paleo time scales ($>10,000$ yrs), changes in the orbital parameters affect
721 the incoming sun light. Figure 14 illustrates the response to a number of orbital
722 solar radiation changes. Incoming radiation (sunlight) typical of the ice age
723 (231k yrs ago) has less incoming sunlight in the Northern Hemispheric summer.
724 However, it has every little annual global mean changes (Fig. 14a) due to increases
725 in sunlight over other regions and seasons. The T_{surf} response pattern in the zonal
726 mean at the different seasons is very similar to the solar forcing, but the response
727 is slightly more zonal and seasonal differences are less dominant (Fig. 14b). The
728 response is also amplified at higher latitudes. However, in the global mean there
729 is no significant global cooling as observed during ice ages. If the solar forcing is
730 combined with a reduction in the CO_2 concentration (from 340ppm to 200ppm),
731 we find a global mean cooling of $-1.7^\circ C$ (Fig. 14c), which is still much weaker than
732 observed during ice ages, but is largely consistent with previous studies of
733 simulations of ice age conditions [Weaver et al. 1998, Braconnot et al. 2007]. This
734 is not unexpected since the GREB model does not include an ice sheet model and,
735 therefore, does not include glacier growth feedbacks that would amplify ice age
736 cycles.

737 A better understanding of the orbital solar radiation forcing can be gained by
738 analysing the response to idealized orbital parameter changes. We therefore vary
739 the Earth distance to the sun (radius), the earth axis tilt to the earth orbit plane
740 (obliquity) and shape of the earth orbit around the sun (eccentricity) over a wider
741 range, see Figs. 14 d-f. When the radius is changed by 10%, the Earth climate
742 becomes essentially uninhabitable, with either global mean temperature above
743 $30^\circ C$ (approx. summer mean temperature of the Sahara) or a completely ice-
744 covered snowball Earth. This suggests that the habitable zone of the Earth radius
745 is fairly small due to the positive feedbacks within the climate system simulated
746 in the GREB model (not considering long-term or more complex atmospheric
747 chemistry feedbacks) and largely consistent with previous studies [Kasting et al.
748 1993].

749 When the obliquity is zero, the tropics become warmer and the polar regions cool
750 down further than today's climate, as they now receive very little sunlight
751 throughout the whole year. In the extreme case, when the obliquity is 90° , the
752 tropics become ice covered and cooler than the polar regions, which are now
753 warmer than the tropics today and ice free. The polar regions now have an
754 extreme seasonal cycle (not shown), with sunlight all day during summer and no
755 sunlight during winter. Any eccentricity increase in amplitude would lead to a
756 warmer overall climate. Thus, a perfect circle orbit around the sun has, on average,
757 the coldest climate and all of the more extreme eccentricity (elliptic) orbits have
758 warmer climates. This suggests that the warming effect of the section of the orbit
759 that has a closer transit around the sun in an eccentricity orbit relative to the
760 perfect circle orbit overcompensates the cooling effect of the more remote transit
761 around the sun in the other half of the orbit relative to the perfect circle orbit.

762 **4. Summary and discussion**

763 In this study, we introduced the MSCM database (version: MSCM-DB v1.0) for
764 research analysis with more than 1,300 experiments. It is based on model
765 simulations with the GREB model for studies of the processes that contribute to
766 the mean climate, the response to doubling of the CO_2 concentration, and different
767 scenarios with CO_2 or solar radiation forcings. The GREB model is a simple climate
768 model that does not simulate internal weather variability, circulation, or cloud
769 cover changes (feedbacks). It provides a simple and fast null hypothesis for the
770 interactions in the climate system and its response to external forcings.

771 The GREB model without flux corrections simulates the mean observed climate
772 well and has an uncertainty of about $10^\circ C$. The model has larger cold biases in the
773 polar regions indicating that the meridional heat transport is not strong enough.
774 Relative to a bare world without any climate processes the RMSE is reduced to
775 about 20-30% relative to observed. Further, the GREB models emissivity function
776 reaches unphysical negative values when water vapour, CO_2 and cloud cover is set
777 to zero. This is a limitation of the log-function parametrization, that can potentially
778 be revised if a new parameterization is developed that considers these cases.
779 However, it is beyond the scope of this study to develop such a new
780 parameterization and it is left for future studies.

781 The MSCM experiments for the conceptual deconstruction of the observed mean
782 climate provide a good understanding of the processes that control the annual
783 mean climate and its seasonal cycle. The cloud cover, atmospheric water vapour,
784 and the ocean heat capacity are the most important processes that determine the
785 regional difference in the annual mean climate and its seasonal cycle. The
786 observed seasonal cycle is strongly damped not only by the ocean heat capacity,
787 but also by the water vapour feedback. In turn, ice-albedo and cloud cover amplify
788 the seasonal cycle in higher latitudes.

789 The conceptual deconstruction of the response to a doubling of the CO_2
790 concentration based on the MSCM experiments has mostly been discussed in
791 DF11, but some additional results shown here focused on the local forcing in
792 response without horizontal interaction. It has been shown here that the CO_2
793 forcing has a clear land-sea contrast, supporting the land-sea contrast in the T_{surf}
794 response. The water vapour feedback is wide-spread and most dominant over the
795 subtropical oceans, whereas the ice-albedo feedback is more localized over
796 Northern Hemispheric continents and around the sea ice border.

797 The series of scenario simulations with CO_2 and solar forcing provide many useful
798 experiments to understand different aspects of the climate response. The RCP and
799 idealized CO_2 forcing scenarios give good insights into the climate sensitivity,
800 regional differences, transient effects, and the role of CO_2 forcing at different
801 seasons or locations. The solar forcing experiments illustrate the subtle
802 differences in the warming pattern to CO_2 forcing and the orbital solar forcing
803 experiments illustrated elements of the climate response to long term, paleo,
804 climate forcings.

805 In summary, the MSCM provides a wide range of experiments for understanding
806 the climate system and its response to external forcings. It builds a basis on which
807 conceptual ideas can be tested to a first-order and it provides a null hypothesis for
808 understanding complex climate interactions. Some of the experiments presented
809 here are similar to previously published simulations. In general, the GREB model
810 results agree well with the results of more complex GCM simulations. It is beyond

811 the scope of this study to discuss all aspects of the experiments and their results.
812 This will be left to future studies. Here we need to keep in mind the limitation that
813 the GREB model does not consider atmospheric or ocean circulation changes nor
814 does it simulate cloud cover feedbacks. Such processes will alter this picture
815 somewhat. The concept of the GREB model may allow to include simple models of
816 atmospheric circulation changes and or formation of cloud cover, and therefore
817 cloud feedbacks. It however, would require further developments of the GREB to
818 include such processes. Currently, studying more detailed regional information of
819 future climate change or social-economical impact studies require more complex
820 climate models.
821 Future development of this MSCM database will continue and it is expected that
822 this database will grow. The development will go in several directions: the GREB
823 model performance in the processes that it currently simulates will be further
824 improved. In particular, the simulation of the hydrological cycle needs to be
825 improved to allow the use of the GREB model to study changes in precipitation.
826 Simulations of aspects of the large-scale atmospheric circulation, aerosols, carbon
827 cycle, or glaciers would further enhance the GREB model and would provide a
828 wider range of experiments to run for the MSCM database.

829 **5. Code and data availability**

830 The MSCM model code, including all required input files, to do all experiments
831 described on the MSCM homepage and in this paper, can be downloaded as
832 compressed tar archive from the MSCM homepage under

833
834 <http://mscm.dkrz.de/download/mscm-web-code.tar.gz>

835

836 or from the bitbucket repository under

837

838 <https://bitbucket.org/tobiasbayr/mscm-web-code>

839

840 The data for all the experiments of the MSCM can be accessed via the MSCM
841 webpage interface (DOI: 10.4225/03/5a8cadac8db60). The mean deconstruction
842 experiments file names have an 11 digits binary code that describe the 11 process
843 switches combination: 1=ON and 0=OFF. The digit from left to right present the
844 following processes:

845

- 846 1. Model corrections
- 847 2. Ice albedo
- 848 3. Cloud cover
- 849 4. Advection of water vapour
- 850 5. Diffusion of water vapour
- 851 6. Hydrologic cycle
- 852 7. Ocean
- 853 8. CO₂
- 854 9. Advection of heat
- 855 10. Diffusion of heat
- 856 11. Atmosphere

857

858 For example, the data file *greb.mean.decon.exp-1011111111.gad* is the
859 experiment with all processes ON, but ice albedo is OFF. The 2x CO₂ response
860 deconstruction experiments file names have a 10 digits binary code that describe
861 the 10 process switches combination. The digit from left to right present the
862 following processes:

- 863
- 864 1. Ocean heat uptake
- 865 2. Advection of water vapour
- 866 3. Diffusion of water vapour
- 867 4. Hydrologic cycle
- 868 5. ice albedo
- 869 6. Advection of heat
- 870 7. Diffusion of heat
- 871 8. Humidity (climatology)
- 872 9. Clouds (climatology)
- 873 10. Topography (Observed)
- 874

875 For example, the data file *response.exp-0111111111.2xCO2.gad* is the experiment
876 with all processes ON, but ocean heat uptake is OFF. The individual experiments
877 can be chosen from the webpage interface by selecting the desired switch
878 combinations. Alternatively, all experiments can be downloaded in a combined
879 tar-file from the webpage interface.

880 For all experiments, the datasets includes five variables: surface, atmospheric and
881 subsurface ocean temperature, atmospheric humidity (column integrated water
882 vapor) and snow/ice cover.

883 **Acknowledgments**

884 This study was supported by the ARC Centre of Excellence for Climate System
885 Science, Australian Research Council (grant CE110001028). The development of
886 the MSCM webpages was support by a number of groups (see [MSCM webpages](#)).
887 Special thanks go to Martin Schweitzer for his work on the first prototype of the
888 MSCM webpages.

889 **References**

- 890 Berger, A., and M. F. Loutre, 1991: Insolation Values for the Climate of the Last
891 10000000 Years. *Quaternary Sci Rev*, **10**, 297-317.
- 892 Bony, S., and Coauthors, 2006: How well do we understand and evaluate climate
893 change feedback processes? *Journal of Climate*, **19**, 3445-3482.
- 894 Bony, S., Stevens, B., Frierson, D. M. W., Jakob, C., Kageyama, M., Pincus, R.,
895 Shepherd, T. G., Sherwood, S. C., Siebesma, A. P., Sobel, A. H., Watanabe, M.,
896 and Webb, M. J., 2015: Clouds, circulation and climate sensitivity, *Nature*
897 *Geosci*, **8**, 261-268.
- 898 Boucher, O., D. Randall, P. Artaxo, C. Bretherton, G. Feingold, P. Forster, V.-M.
899 Kerminen, Y. Kondo, H. Liao, U. Lohmann, P. Rasch, S.K. Satheesh, S.
900 Sherwood, B. Stevens and X.Y. Zhang, 2013: Clouds and Aerosols. In:
901 Climate Change 2013: The Physical Science Basis. Contribution of
902 Working Group I to the Fifth Assessment Report of the Intergovernmental
903 Panel on Climate Change [Stocker, T.F., D. Qin, G.-K. Plattner, M. Tignor,
904 S.K. Allen, J. Boschung, A. Nauels, Y. Xia, V. Bex and P.M. Midgley (eds.)].
905 Cambridge University Press, Cambridge, United Kingdom and New York,
906 NY, USA.
- 907 Braconnot, P., and Coauthors, 2007: Results of PMIP2 coupled simulations of the
908 Mid-Holocene and Last Glacial Maximum - Part 1: experiments and large-
909 scale features. *Clim Past*, **3**, 261-277.
- 910 Cess, R. D., and Coauthors, 1993: Uncertainties in Carbon-Dioxide Radiative
911 Forcing in Atmospheric General-Circulation Models. *Science*, **262**, 1252-
912 1255.
- 913 Cubasch, U., R. Voss, G. C. Hegerl, J. Waszkewitz, and T. J. Crowley, 1997:
914 Simulation of the influence of solar radiation variations on the global
915 climate with an ocean-atmosphere general circulation model. *Climate*
916 *Dynamics*, **13**, 757-767.
- 917 Donohoe, A., D. M. W. Frierson, and D. S. Battisti, 2014: The effect of ocean mixed
918 layer depth on climate in slab ocean aquaplanet experiments. *Clim. Dyn.*, **43**,
919 1041-1055, doi:10.1007/s00382-013-1843-4.
- 920 Dommenget, D., 2012: Analysis of the Model Climate Sensitivity Spread Forced
921 by Mean Sea Surface Temperature Biases. *Journal of Climate*, **25**, 7147-
922 7162.
- 923 Dommenget, D., and J. Floter, 2011: Conceptual understanding of climate change
924 with a globally resolved energy balance model. *Climate Dynamics*, **37**,
925 2143-2165.
- 926 Forster, P. M., T. Andrews, P. Good, J. M. Gregory, L. S. Jackson, and M. Zelinka,
927 2013: Evaluating adjusted forcing and model spread for historical and
928 future scenarios in the CMIP5 generation of climate models. *Journal of*
929 *Geophysical Research-Atmospheres*, **118**, 1139-1150.
- 930 Goosse, H., and Coauthors, 2010: Description of the Earth system model of
931 intermediate complexity LOVECLIM version 1.2. *Geosci Model Dev*, **3**, 603-
932 633.
- 933 Hansen, J., M. Sato, and R. Ruedy, 1997: Radiative forcing and climate response.
934 *Journal of Geophysical Research-Atmospheres*, **102**, 6831-6864.

935 Held, I. M., M. Winton, K. Takahashi, T. Delworth, F. R. Zeng, and G. K. Vallis, 2010:
936 Probing the Fast and Slow Components of Global Warming by Returning
937 Abruptly to Preindustrial Forcing. *Journal of Climate*, **23**, 2418-2427.

938 Huybers, P., 2006: Early Pleistocene glacial cycles and the integrated summer
939 insolation forcing. *Science*, **313**, 508-511.

940 Kalnay, E., and Coauthors, 1996: The NCEP/NCAR 40-year reanalysis project.
941 *Bulletin of the American Meteorological Society*, **77**, 437-471.

942 Kang, S. M., R. Seager, D. M. W. Frierson, and X. Liu, 2015: Croll revisited: Why is
943 the northern hemisphere warmer than the southern hemisphere? *Clim. Dyn.*,
944 **44**, 1457–1472, doi:10.1007/s00382-014-2147-z.

945 Kasting, J. F., D. P. Whitmire, and R. T. Reynolds, 1993: Habitable Zones around
946 Main-Sequence Stars. *Icarus*, **101**, 108-128.

947 Kiehl, J. T., and V. Ramanathan, 1982: Radiative Heating Due to Increased Co₂ -
948 the Role of H₂O Continuum Absorption in the 12-18 Mu-M Region. *Journal*
949 *of the Atmospheric Sciences*, **39**, 2923-2926.

950 Knutti, R., G. A. Meehl, M. R. Allen, and D. A. Stainforth, 2006: Constraining
951 climate sensitivity from the seasonal cycle in surface temperature. *Journal*
952 *of Climate*, **19**, 4224-4233.

953 Lorbacher, K., D. Dommenges, P. P. Niiler, and A. Kohl, 2006: Ocean mixed layer
954 depth: A subsurface proxy of ocean-atmosphere variability. *Journal of*
955 *Geophysical Research-Oceans*, **111**, -.

956 Meehl, G. A., J. M. Arblaster, K. Matthes, F. Sassi, and H. van Loon, 2009:
957 Amplifying the Pacific Climate System Response to a Small 11-Year Solar
958 Cycle Forcing. *Science*, **325**, 1114-1118.

959 Myhre, G., E. J. Highwood, K. P. Shine, and F. Stordal, 1998: New estimates of
960 radiative forcing due to well mixed greenhouse gases. *Geophysical*
961 *Research Letters*, **25**, 2715-2718.

962 Peixoto, J. P. and A. H. O., 1992: *Physics of Climate*. Springer US,.

963 Petoukhov, V., A. Ganopolski, V. Brovkin, M. Claussen, A. Eliseev, C. Kubatzki, and
964 S. Rahmstorf, 2000: CLIMBER-2: a climate system model of intermediate
965 complexity. Part I: model description and performance for present
966 climate. *Climate Dynamics*, **16**, 1-17.

967 Roeckner, E., and Coauthors, 2003: The atmospheric general circulation model
968 ECHAM 5. Part I: Model description. *Reports of the Max-Planck-Institute*
969 *for Meteorology*, **349**.

970 Rossow, W. B., and R. A. Schiffer, 1991: Isccp Cloud Data Products. *Bulletin of the*
971 *American Meteorological Society*, **72**, 2-20.

972 Rossow, W. B., and Y. C. Zhang, 1995: Calculation of Surface and Top of
973 Atmosphere Radiative Fluxes from Physical Quantities Based on Isccp
974 Data Sets .2. Validation and First Results. *Journal of Geophysical Research-*
975 *Atmospheres*, **100**, 1167-1197.

976 Smith, R. S., J. M. Gregory, and A. Osprey, 2008: A description of the FAMOUS
977 (version XDBUA) climate model and control run, *Geosci. Model Dev.*, **1**,
978 53-68.

979 Taylor, K. E., R. J. Stouffer, and G. A. Meehl, 2012: An Overview of Cmp5 and the
980 Experiment Design. *Bulletin of the American Meteorological Society*, **93**,
981 485-498.

982 van Vuuren, D. P., and Coauthors, 2011: The representative concentration
983 pathways: an overview. *Climatic Change*, **109**, 5-31.

984 Weaver, A. J., M. Eby, F. F. Augustus, and E. C. Wiebe, 1998: Simulated influence of
985 carbon dioxide, orbital forcing and ice sheets on the climate of the Last
986 Glacial Maximum. *Nature*, **394**, 847-853.

987 Weaver, A. J., and Coauthors, 2001: The UVic Earth System Climate Model: Model
988 description, climatology, and applications to past, present and future
989 climates. *Atmosphere-Ocean*, **39**, 361-428.

990 Willson, R. C., and H. S. Hudson, 1991: The Sun's Luminosity over a Complete
991 Solar-Cycle. *Nature*, **351**, 42-44.

992 Yang, H., Q. Li, K. Wang, Y. Sun, and D. Sun, 2015: Decomposing the meridional
993 heat transport in the climate system. *Clim. Dyn.*, **44**, 2751-2768,
994 doi:10.1007/s00382-014-2380-5.

995

996

997 **Appendix A1: GREB model equations**

998 The GREB model has four primary prognostic equations given below and all
999 variable names are listed and explained in Table A1. The surface temperature,
1000 T_{surf} , tendencies:

$$1001 \gamma_{surf} \frac{dT_{surf}}{dt} = F_{solar} + F_{thermal} + F_{latent} + F_{sense} + F_{ocean} + F_{correct} \quad [A1]$$

1002
1003 The atmospheric layer temperature, T_{atmos} , tendencies:

$$1004 \gamma_{atmos} \frac{dT_{atmos}}{dt} = -F_{sense} + F_{a_{thermal}} + Q_{latent} \\ 1005 + \gamma_{atmos} (\kappa \cdot \nabla^2 T_{atmos} - \vec{u} \cdot \nabla T_{atmos}) \quad [A2]$$

1006
1007 The subsurface ocean temperature, T_{ocean} , tendencies:

$$1008 \frac{dT_{ocean}}{dt} = \frac{1}{\Delta t} \Delta T_{o_{entrain}} - \frac{1}{\gamma_{ocean} - \gamma_{surf}} F_{o_{sense}} + F_{o_{correct}} \quad [A3]$$

1009
1010 The atmospheric specific humidity, q_{air} , tendencies:

$$1011 \frac{dq_{air}}{dt} = \Delta q_{eva} + \Delta q_{precip} + \kappa \cdot \nabla^2 q_{air} - \vec{u} \cdot \nabla q_{air} + q_{correct} \quad [A4]$$

1012 It should be noted here that heat transport is only within the atmospheric layer
1013 (eq. [A2]). Together with the moisture transport in eq. [A4] these transports are
1014 the only way in which grid points of the GREB model interact with each other in
1015 the horizontal directions.

1016 The surface layer heat capacity, γ_{surf} , is constant over land points. For ocean
1017 points it follows the ocean mixed layer depth, h_{mld} , if T_{surf} is above a temperature
1018 range near freezing. Within a range below freezing it is a linear increasing function
1019 of T_{surf} and for T_{surf} below this range γ_{surf} the same as over land points. (see
1020 DF11).

1021 The absorbed solar radiation, F_{solar} , is a function of the cloud cover, CLD , boundary
1022 condition and the surface albedo, α_{surf} :

$$1023 F_{solar} = (1 - \alpha_{clouds}) \cdot (1 - \alpha_{surf}) \cdot S_0 \cdot r \quad [A5]$$

1024 with the atmospheric albedo, $\alpha_{clouds} = 0.35 \cdot CLD$. α_{surf} is a global constant if
1025 T_{surf} is below or above a temperature range near freezing. Within this range it is
1026 a linear decreasing function of T_{surf} , (see DF11). The thermal radiation at the
1027 surface is

$$1028 F_{thermal} = -\sigma T_{surf}^4 + \varepsilon_{atmos} \sigma T_{atmos-rad}^4 \quad [A6]$$

1029 and the thermal radiation from the atmosphere is

1040
1041

1042 $Fa_{thermal} = \sigma T_{surf}^4 - 2\varepsilon_{atmos}\sigma T_{atmos-rad}^4$ [A7]

1043

1044 The emissivity of the atmosphere, ε_{atmos} , is a function of the cloud cover, CLD ,
 1045 the atmospheric water vapour, $viwv_{atmos}$, and the CO₂, CO_2^{topo} , concentration

1046

1047 $\varepsilon_{atmos} = \frac{pe_8 - CLD}{pe_9} \cdot (\varepsilon_0 - pe_{10}) + pe_{10}$ [A8]

1048

1049 with

1050

1051 $\varepsilon_0 = pe_4 \cdot [pe_1 \cdot CO_2^{topo} + pe_2 \cdot viwv_{atmos} + pe_3]$
 1052 $+ pe_5 \cdot [pe_1 \cdot CO_2^{topo} + pe_3] + pe_6 \cdot [pe_2 \cdot viwv_{atmos} + pe_3] + pe_7$ [A9]

1053

1054 The first three terms in the eq. [A9] represent different spectral bands in which
 1055 the thermal radiation of water vapour and the CO₂ are active. In the first term both
 1056 are active, in the second only CO₂ and in the third only water vapour. The
 1057 combined effect of eqs. [A8] and [A9] is that the sensitivity of the emissivity to CO₂
 1058 is depending on the presents of cloud cover and water vapour.

1059 It is important to note that this log-function parametrization of the emissivity is
 1060 an approximation developed in DF11 for 2xCO₂-concentration experiments. While
 1061 the parametrization may be a good approximation for a wide range of the
 1062 greenhouse gasses, it is likely to have limited skill in extreme variation of the
 1063 greenhouse gasses. For instance, if all greenhouse gasses (CO₂ and water vapour)
 1064 concentrations and cloud cover are zero then the emissivity of the atmospheric
 1065 layer in eq. [A9] becomes -0.26. This is not a physically meaningful value and
 1066 experiments in which all greenhouse gasses (CO₂ and water vapour) and cloud
 1067 cover are zero need to be analysed with caution. The analysis section will discuss
 1068 these limitations in these experiments.

1069 **Tables**

1070

1071 **Table 1:** Processes (switches) controlled in the sensitivity experiment for the
 1072 mean climate deconstruction. Indentation in the left column indicates processes
 1073 switches are dependent on the switches above being ON.

Mean Climate Deconstruction	
Name	Description
Ice-albedo	controls surface albedo (α_{surf}) and heat capacity (γ_{surf}) at sea ice points as function of T_{surf}
Clouds	controls cloud cover climatology. OFF equals no clouds.
Oceans	controls F_{ocean} term in eq. [A1] and the heat capacity (γ_{surf}) off all ocean points. OFF equals no F_{ocean} and as γ_{surf} over land.
Atmosphere	controls sensible heat flux (F_{sense}) and the downward atmospheric thermal radiation term in eq. [A6].
Diffusion of Heat	controls diffusion of heat
Advection of Heat	controls advection of heat
CO ₂	controls CO ₂ concentration
Hydrological cycle	controls atmospheric humidity. OFF equals zero humidity
Diffusion of water vapour	controls diffusion of water vapour
Advection of water vapour	controls advection of water vapour
Model Corrections	controls model flux correction terms

1074

1075

1076

1077

1078 **Table 2:** Processes (switches) controlled in the sensitivity experiment for the
 1079 $2\times\text{CO}_2$ response deconstruction. Indentation in the left column indicates
 1080 processes switches are dependent on the switches above being ON.
 1081

2xCO ₂ Response Deconstruction	
Boundary Conditions	
Name	Description
Topography (Observed)	controls topography effect on thermal radiation. OFF equals all land point on sea level.
Clouds (climatology)	controls cloud cover climatology. OFF equals 0.7 cloud cover everywhere.
Humidity (climatology)	controls the humidity constraint. OFF equals a control humidity 0.0052 [kg/kg] everywhere. Humidity can still respond to forcings.
Feedbacks/Processes	
Diffusion of Heat	controls diffusion of heat
Advection of Heat	controls advection of heat
Ice-albedo	controls surface albedo (α_{surf}) and heat capacity (γ_{surf}) at sea ice points as function of T_{surf}
Ocean heat uptake	controls F_{ocean} term in eq. [A1] and the heat capacity (γ_{surf}) off all ocean points. OFF equals no F_{ocean} and γ_{surf} of a 50m water column.
Hydrological cycle	controls atmospheric humidity. OFF equals zero humidity
Diffusion of water vapour	controls diffusion of water vapour
Advection of water vapour	controls advection of water vapour

1082

1083

1084

1085

1086 **Table 3:** List of scenario experiments.

RCP CO ₂ -scenarios		
Name	length	Description
Historical	1850-2000	CO ₂ -concentration following the historical scenario
RCP8.5	2001-2100	CO ₂ -concentration following the RCP8.5 scenario
RCP6	2001-2100	CO ₂ -concentration following the RCP6 scenario
RCP4	2001-2100	CO ₂ -concentration following the RCP4 scenario
RCP3PD	2001-2100	CO ₂ -concentration following the RCP3PD scenario
A1B	2001-2100	CO ₂ -concentration following the A1B scenario
Idealized CO ₂ concentrations		
Zero-CO ₂	100yrs	zero CO ₂ concentrations
0.5xCO ₂	50yrs	140ppm CO ₂ concentrations
2xCO ₂	50yrs	560ppm CO ₂ concentrations
4xCO ₂	100yrs	1120ppm CO ₂ concentrations
10xCO ₂	100yrs	2800ppm CO ₂ concentrations
2xCO ₂ abrupt reverse	100yrs	as 2xCO ₂ with an abrupt reverse to control after 30yrs
2xCO ₂ wave	100yrs	CO ₂ concentration oscillating with 30yrs period
Partial CO ₂ concentrations		
CO ₂ -N-hemis	50yrs	2xCO ₂ only in the northern hemisphere
CO ₂ -S-hemis	50yrs	2xCO ₂ only in the southern hemisphere
CO ₂ -tropics	50yrs	2xCO ₂ only between 30°S and 30°N
CO ₂ -extra-tropics	50yrs	2xCO ₂ only poleward of 30°
CO ₂ -oceans	50yrs	2xCO ₂ only over ice-free ocean points
CO ₂ -land	50yrs	2xCO ₂ only over land and sea ice points
CO ₂ -winter	50yrs	2xCO ₂ only in the month Oct. to Mar.
CO ₂ -summer	50yrs	2xCO ₂ only in the month Apr. to Sep.
Solar radiation		
solar+27W/m ²	50yrs	solar constant increased by +27W/m ²
11yrs-solar	50yrs	solar idealized solar constant 11yrs cycle
Orbital parameter		
Solar-231Kyr	100yrs	incoming solar radiation according to orbital parameters 231Kyr ago.
Solar-231Kyr-200ppm	100yrs	as Solar-231Kyr, but with CO ₂ concentrations decreased from 280ppm to 200ppm.
Orbit-radius	40steps	equilibrium response to different Earth orbit radius from 0.8AU to 1.2AU.
Obliquity	45steps	equilibrium response to different Earth axis tilt from -25° to 90°
Eccentricity	60steps	equilibrium response to different Earth orbit eccentricity from 0.3 to 0.3

1087

1088

1089

Table A1: Variables of the GREB model equations.

Variable	Dimensions	Description
T_{surf}	x, y, t	surface temperature
T_{atmos}	x, y, t	atmospheric temperature
T_{ocean}	x, y, t	subsurface ocean temperature
q_{air}	x, y, t	atmospheric humidity
γ_{surf}	x, y, t	heat capacity of the surface layer
γ_{atmos}	x, y, t	heat capacity of the atmosphere
γ_{ocean}	x, y, t	heat capacity of the subsurface ocean
F_{solar}	x, y, t	solar radiation absorbed at the surface
$F_{thermal}$	x, y, t	thermal radiation into the surface
$F_{a_{thermal}}$	x, y, t	thermal radiation into the atmospheric
F_{latent}	x, y, t	latent heat flux into the surface
Q_{latent}	x, y, t	latent heat flux into the atmospheric
F_{sense}	x, y, t	sensible heat flux from the atmosphere into the surface
$F_{O_{sense}}$	x, y, t	sensible heat flux from the subsurface ocean into the surface layer
F_{ocean}	x, y, t	sensible heat flux from the subsurface ocean
$F_{correct}$	x, y, t	heat flux corrections for the surface
$F_{O_{correct}}$	x, y, t	heat flux corrections for the subsurface ocean
$q_{correct}$	x, y, t	mass flux corrections for the atmospheric humidity
$\Delta T_{O_{entrain}}$	x, y, t	subsurface ocean temperature tendencies by entrainment
Δq_{eva}	x, y, t	mass flux for the atmospheric humidity by evaporation
Δq_{precip}	x, y, t	mass flux for the atmospheric humidity by precipitation
α_{surf}	x, y, t	albedo of the surface layer
ϵ_{atmos}	x, y, t	emissivity of the atmosphere
$T_{atmos-rad}$	x, y, t	atmospheric radiation temperature
$viwv_{atmos}$	x, y, t	atmospheric column water vapour mass
κ	constant	isotropic diffusion coefficient
pe_i	constant	empirical emissivity function parameters
\vec{u}	x, y, t _j	horizontal wind field
α_{clouds}	x, y, t _j	albedo of the atmosphere
h_{mld}	x, y, t _j	Ocean mixed layer depth
r	y, t _j	fraction of incoming sunlight (24hrs average)
CO_2^{topo}	x, y	CO_2 concentration scaled by topographic elevation
S_0	constant	solar constant
σ	constant	Stefan-Bolzman constant
t _j	-	day within the annual calendar
Δt	constant	model integration time step
σ	constant	Stefan-Boltzmann constant

1092 **Figures**

1093

1094 **Figure 1.** MSCM interface running the deconstruction of the mean climate
1095 experiments. The experiment A, on the left, has all processes turned ON
1096 and experiment B, on right, has all turned OFF. The T_{surf} of Experiment A is
1097 shown in the upper left map, Exp. B in the upper right and the difference
1098 between both in the lower map. The example shows the values for the
1099 October mean.

1100

1101 **Figure 2.** MSCM interface running the deconstruction of the response to a
1102 doubling of the CO_2 concentration experiments. The experiment A, on the
1103 left, has all processes turned ON and experiment B, on right, has all turned
1104 OFF. The T_{surf} response of Experiment A is shown in the upper left map, Exp.
1105 B in the upper right and the difference between both in the lower map. The
1106 example shows the annual mean values after 28yrs.

1107

1108 **Figure 3.** Examples of the MSCM scenario interface. (a) presenting a single
1109 scenario (here RCP 8.5 CO_2 forcing) and (b) the comparison of two different
1110 scenarios (here a CO_2 forcing is compared against a change in the solar
1111 constant by $+27W/m^2$).

1112

1113 **Figure 4.** T_{surf} annual mean (upper row) and seasonal cycle (half the
1114 difference between mean of July to September minus January to March;
1115 middle row) for the GREB experiment with all processes turned OFF (Bare
1116 Earth), only the correction term OFF (GREB) and observed (identical to
1117 GREB with all processes on) are shown. The zonal mean of the annual mean
1118 (g) and seasonal cycle (h) of the experiments and observations in
1119 comparison with the zonal mean RMSE of the GREB model without
1120 correction terms relative to observed are shown.

1121

1122 **Figure 5.** Changes in the annual mean T_{surf} in the GREB model simulations
1123 with different processes turned OFF as described in section 2a relative to
1124 the complete GREB model without model correction terms: (a) Ice/Snow,
1125 (b) clouds, (c) oceans, (d) heat advection, (e) heat diffusion, (f) CO_2
1126 concentration, (g) hydrological cycle, (h) diffusion of water vapour and (i)
1127 advection of water vapour. Global mean differences are shown in the
1128 headings. Differences are for the control minus the sensitivity experiment
1129 (positive indicates the control experiment is warmer). All values are in $^{\circ}C$.
1130 In some panels, the values are scaled for better comparison: (b), (c) and (f)
1131 by a factor of 2, (a), (d) and (e) by a factor of 3, and (h) and (i) by a factor
1132 of 6.

1133

1134 **Figure 6.** As in Fig. 5, but for the seasonal cycle. The mean seasonal cycle is
1135 defined by the difference between the month [JAS] - [JFM] divided by two.
1136 Positive values on the North hemisphere indicate stronger seasonal cycle
1137 in the sensitivity experiments than in the full GREB model. Vice versa for
1138 the Southern Hemisphere. Global root mean square differences are shown
1139 in the headings. All values are in $^{\circ}C$. In some panels, the values are scaled
1140 for better comparison: (b), (d) and (e) by a factor of 2, and (h) and (i) by a

1141 factor of 10. (g) is the mean for the hydrological cycle experiments with and
1142 without the ice-albedo process active.

1143
1144 **Figure 7.** Zonal mean values of the annual mean (a) and seasonal cycle
1145 differences (b) for the experiments as shown in Figs. 5 and 6. g) The mean
1146 for the hydrological cycle is for the experiments with and without the ice-
1147 albedo process active.

1148
1149 **Figure 8.** Conceptual build-up of the annual mean climate: starting with all
1150 processes turned OFF (a) and then adding more processes in each row: (b)
1151 atmosphere, (d) CO₂, (f) oceans, (h) heat diffusion, (j) heat advection, (l)
1152 hydrological cycle, (n) ice-albedo, (p) clouds and (r) water vapour
1153 transport. The panels on the right column show the difference of the left
1154 panel to the previous row left panel. Global mean values are shown in the
1155 heading. All values are in °C. In some panels in the right column the values
1156 are scaled for better comparison: (e), (g) and (q) by a factor of 2, (i) by a
1157 factor of 3 and (k), (o) and (s) by a factor of 4. For details see on the
1158 experiments see section 2a.

1159
1160 **Figure 9.** As in Fig. 8, but conceptual build-up of the seasonal cycle. The
1161 seasonal cycle is defined by the difference between the month [JAS] - [JFM]
1162 divided by two. Global mean absolute values are shown in the heading. In
1163 some panels in the right column the values are scaled for better
1164 comparison: (c), (i), (m) and (o) by a factor of 2, (k), (q) and (s) by a factor
1165 of 5 and for (e) by a factor of 30.

1166
1167 **Figure 10.** Local T_{surf} response to doubling of the CO₂ concentration in
1168 experiments without atmospheric transport (each point on the maps is
1169 independent of the others). (a) GREB with topography, humidity and cloud
1170 processes and all other processes OFF. (b) Difference of (a) to GREB with
1171 topography and all other processes OFF scaled by a factor of 10. (c) GREB
1172 model as in (a), but with ice-albedo process ON. (d) Difference of (c)-(a)
1173 scaled by a factor of 2. (e) GREB model as in (a), but with hydrological cycle
1174 process ON. (f) Difference of (e)-(a) scaled by a factor of 2. For details see
1175 on the experiments see section 2b.

1176
1177 **Figure 11.** Global mean T_{surf} response to idealized forcing scenarios: (a)
1178 different RCP CO₂ forcing scenarios. (b) Scaled CO₂ concentrations. (c)
1179 idealized CO₂ concentration time evolutions (dotted lines) and the
1180 respective T_{surf} responses (solid lines of the same colour) for the 2xCO₂
1181 abrupt reverse (red) and the 2xCO₂ wave (blue) simulations. (d) idealized
1182 11yrs solar cycle. List of experiments is given in Table 3.

1183
1184 **Figure 12.** T_{surf} response to partial doubling of the CO₂ concentration in:
1185 Northern (a) and Southern (b) hemisphere, tropics (d) and extra-tropics
1186 (e), oceans (g) and land (h), and in boreal winter (j) and summer (k) . The
1187 right column panels show the difference between the two panels two the
1188 left in the same row.

1189

1190 **Figure 13.** T_{surf} response to changes in the solar constant by $+27\text{W/m}^2$
1191 (middle column) versus a doubling of the CO_2 concentration (left column)
1192 for the annual mean (upper) and the seasonal cycle (lower). The seasonal
1193 cycle is defined by the difference between the month [JAS] - [JFM] divided
1194 by two. The right column panels show the difference between the two
1195 panels two the left in the same row scaled by 4 (c) and 3 (f).

1196 **Figure 14.** Orbital parameter forcings and T_{surf} responses: (a) incoming
1197 solar radiation changes in the Solar-231Kyr experiment relative to the
1198 control GREB model. T_{surf} response in Solar-231Kyr (b) and Solar-231Kyr-
1199 200ppm (c) relative to the control GREB model. Annual mean T_{surf} in Orbit-
1200 radius (d), Obliquity (e) and Eccentricity (f). The solid vertical line in (d)-
1201 (f) marks the control (today) GREB model.

1202 **Supplementary Figures**

1203
1204 **SFigure 1.** Changes in the annual mean T_{surf} in the GREB model
1205 simulations with different processes turn OFF as in Fig. 5 but relative to the
1206 complete GREB model without model correction terms and without
1207 Ice/Snow: (a) undefined, (b) clouds, (c) oceans, (d) heat advection, (e) heat
1208 diffusion, (f) CO_2 concentration, (g) hydrological cycle, (h) diffusion of
1209 water vapour and (i) advection of water vapour. Global mean differences
1210 are shown in the headings. All values are in $^{\circ}\text{C}$. In some panels, the values
1211 are scaled for better comparison: (a), (d) and (e) by a factor of 2, and (h)
1212 and (i) by a factor of 5.

1213
1214 **SFigure 2.** Conceptual build-up of the annual mean climate as in Fig. 8.
1215 Panels (a) to (c) as in fig.8. (d) with the atmospheric emissivity set to zero,
1216 and (f) with the emissivity set 0.01. The panels on the right column show
1217 the difference of the left panel to (a). Global mean values are shown in the
1218 heading. All values are in $^{\circ}\text{C}$. In the right column, the values are scaled by a
1219 factor of 2 for better comparison. For details see on the experiments see
1220 section 2a.

1221
1222

Figure 1

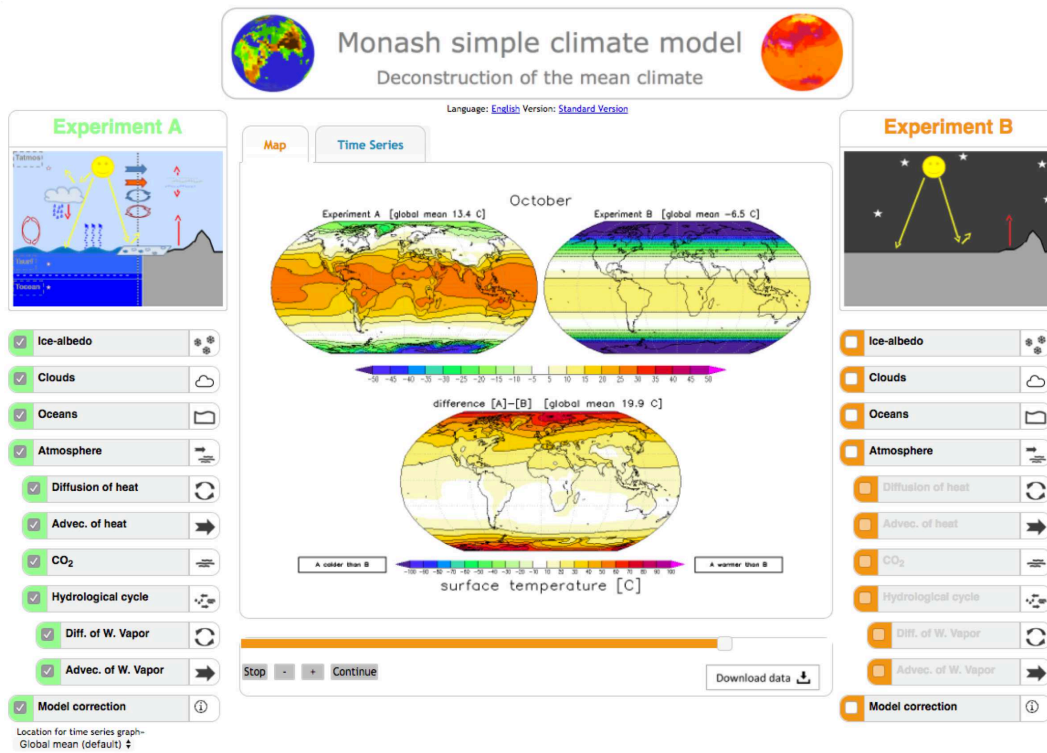


Figure 1: MSCM interface running the deconstruction of the mean climate experiments. The experiment A, on the left, has all processes turned ON and experiment B, on right, has all turned OFF. The T_{surf} of Experiment A is shown in the upper left map, Exp. B in the upper right and the difference between both in the lower map. The example shows the values for the October mean.

Figure 2

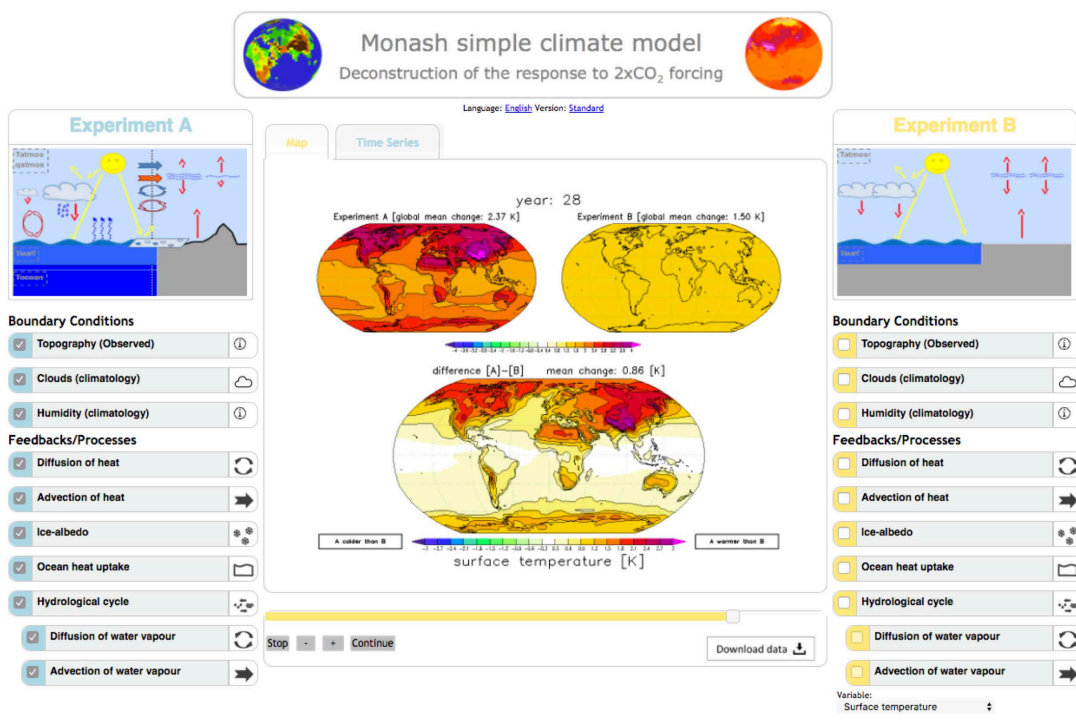
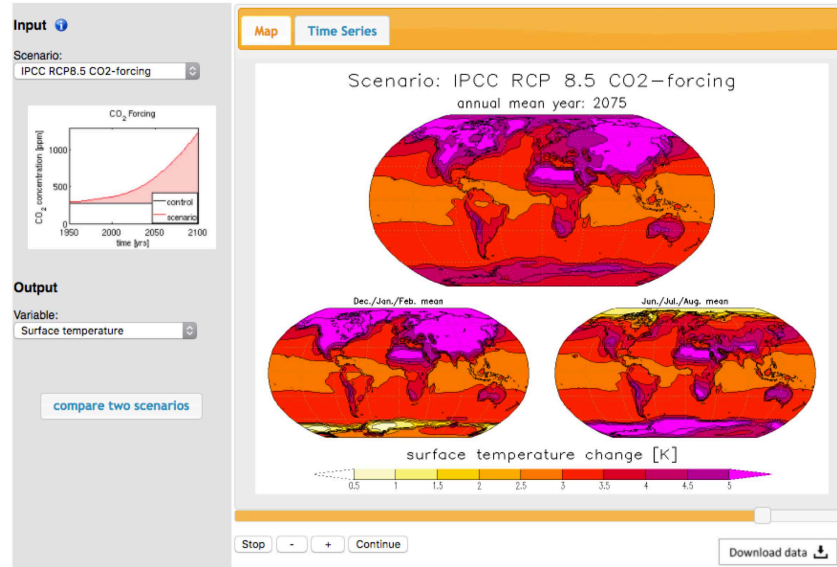


Figure 2: MSCM interface running the deconstruction of the response to a doubling of the CO_2 concentration experiments. The experiment A, on the left, has all processes turned ON and experiment B, on right, has all turned OFF. The T_{surf} response of Experiment A is shown in the upper left map, Exp. B in the upper right and the difference between both in the lower map. The example shows the annual mean values after 28yrs.

Figure 3

(a)



(b)

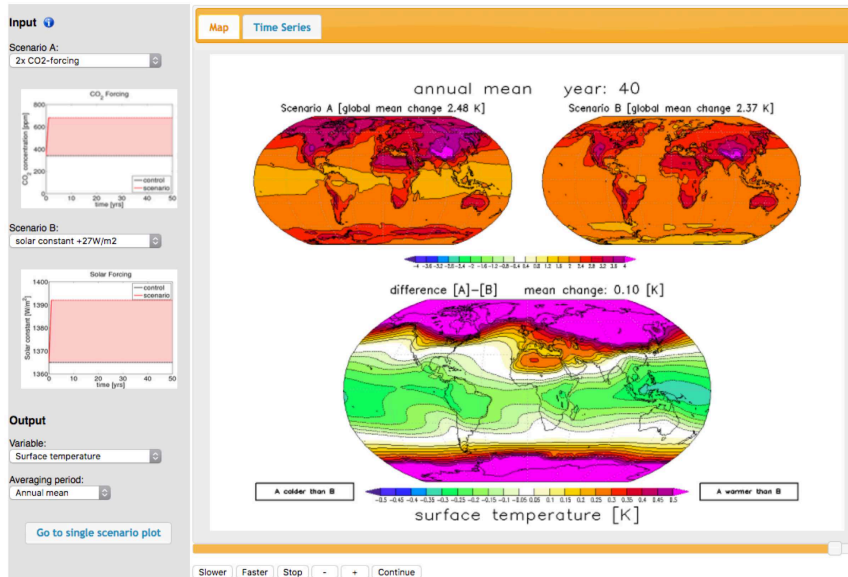


Figure 3: Examples of the MSCM scenario interface. (a) presenting a single scenario (here RCP 8.5 CO_2 forcing) and (b) the comparison of two different scenarios (here a CO_2 forcing is compared against a change in the solar constant by $+27W/m^2$).

Figure 4

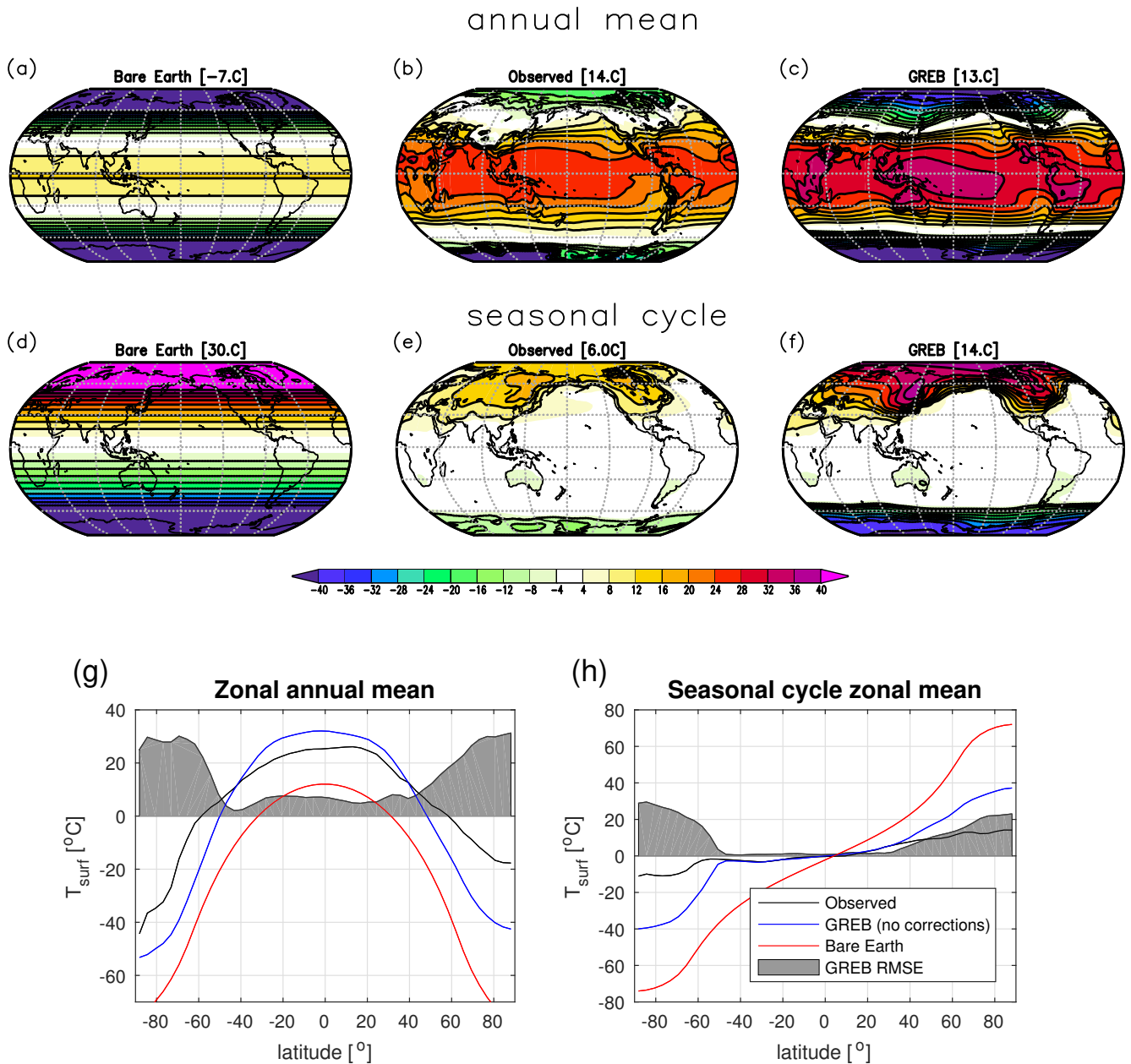


Figure 4: T_{surf} annual mean (upper row) and seasonal cycle (half the difference between mean of July to September minus January to March; middle row) for the GREB experiment with all processes turned OFF (Bare Earth), only the correction term OFF (GREB) and observed (identical to GREB with all processes on) are shown. The zonal mean of the annual mean (g) and seasonal cycle (h) of the experiments and observations in comparison with the zonal mean RMSE of the GREB model without correction terms relative to observed are shown.

Figure 5

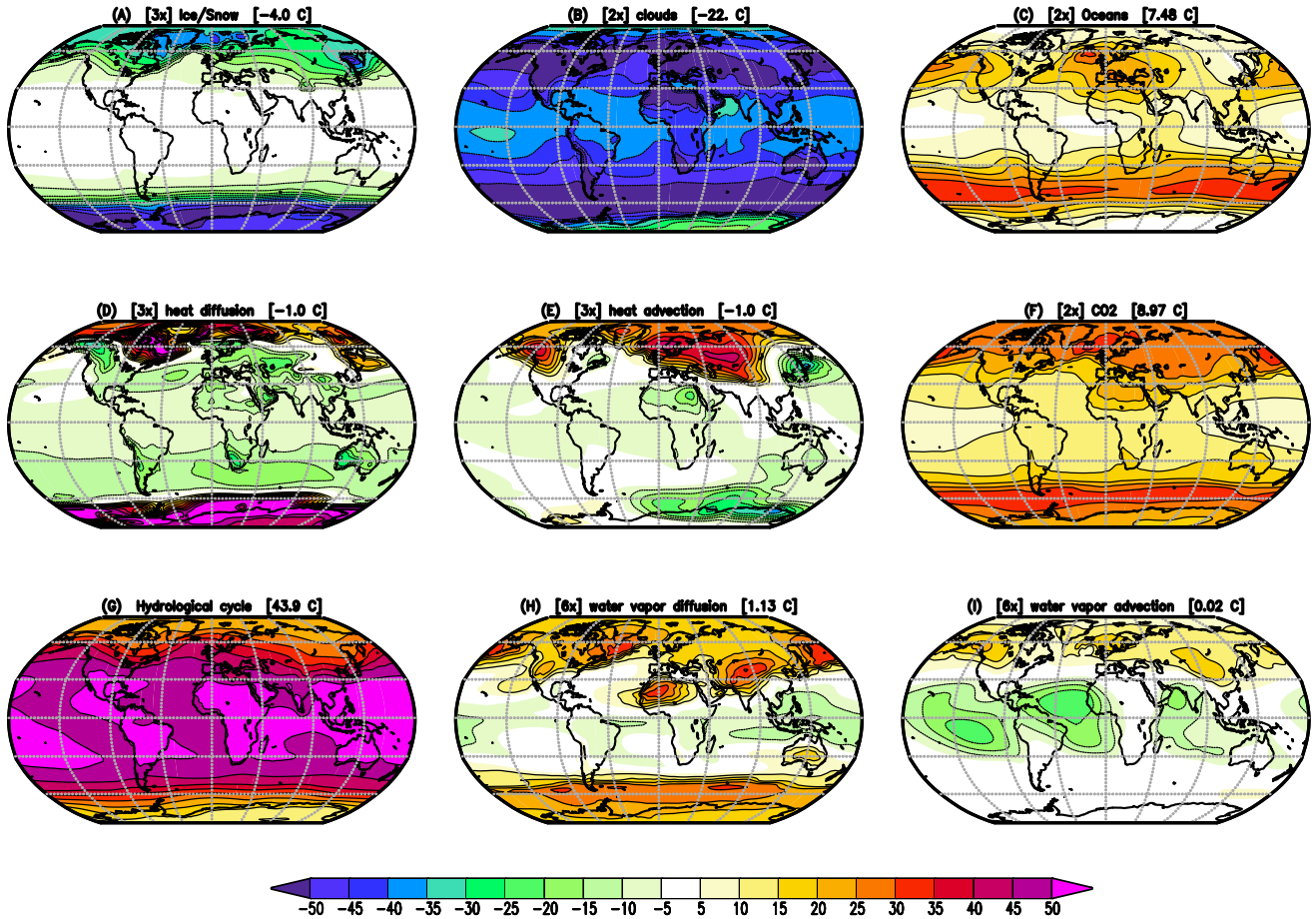


Figure 5: Changes in the annual mean T_{surf} in the GREB model simulations with different processes turned OFF as described in section 2a relative to the complete GREB model without model correction terms: (a) Ice/Snow, (b) clouds, (c) oceans, (d) heat advection, (e) heat diffusion, (f) CO_2 concentration, (g) hydrological cycle, (h) diffusion of water vapour and (i) advection of water vapour. Global mean differences are shown in the headings. Differences are for the control minus the sensitivity experiment (positive indicates the control experiment is warmer). All values are in $^{\circ}C$. In some panels, the values are scaled for better comparison: (b), (c) and (f) by a factor of 2, (a), (d) and (e) by a factor of 3, and (h) and (i) by a factor of 6.

Figure 6

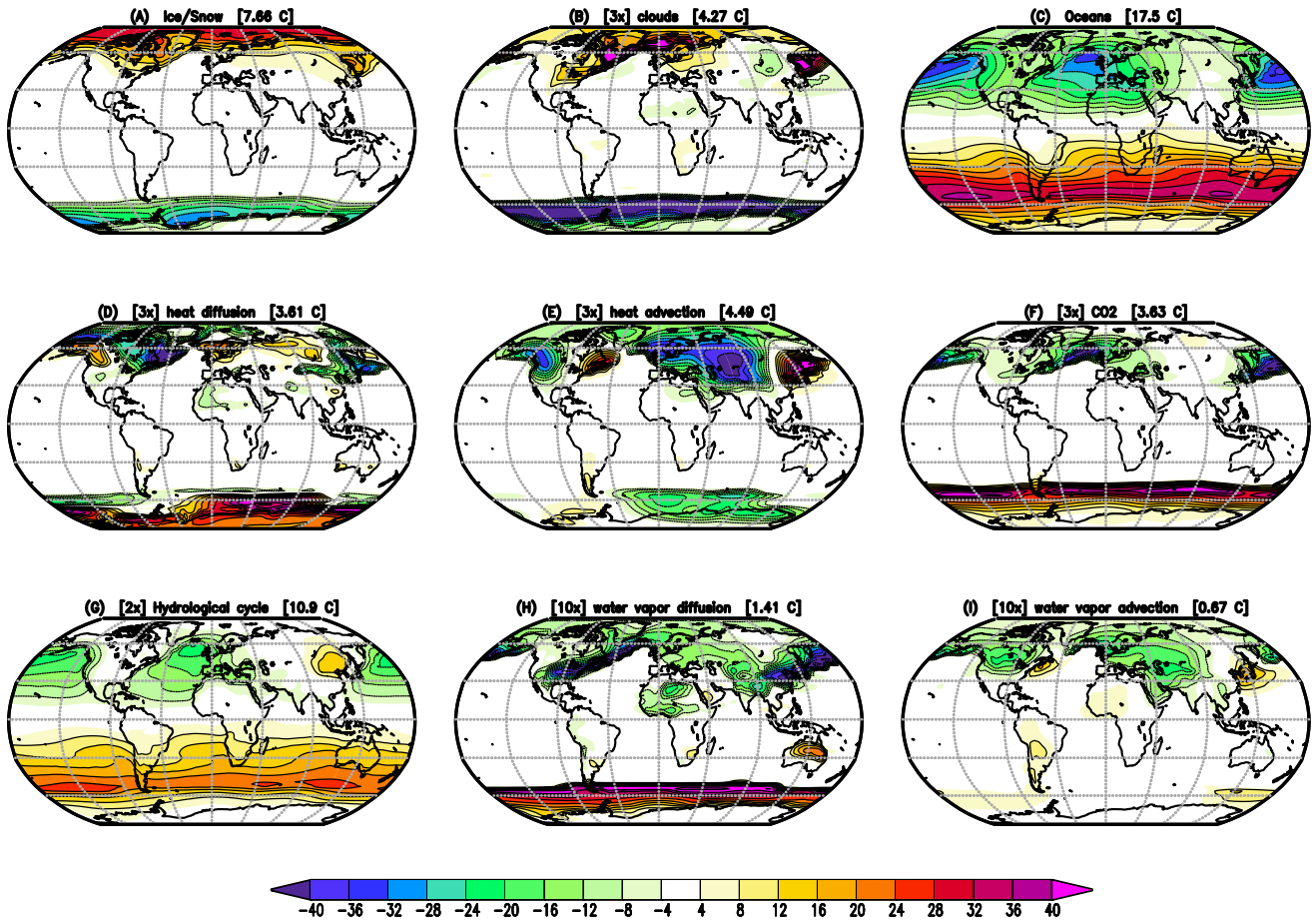


Figure 6: As in Fig. 5, but for the seasonal cycle. The mean seasonal cycle is defined by the difference between the month [JAS] - [JFM] divided by two. Positive values on the North hemisphere indicate stronger seasonal cycle in the sensitivity experiments than in the full GREB model. Vice versa for the Southern Hemisphere. Global root mean square differences are shown in the headings. All values are in $^{\circ}C$. In some panels, the values are scaled for better comparison: (b), (d) and (e) by a factor of 2, and (h) and (i) by a factor of 10. (g) is the mean for the hydrological cycle experiments with and without the ice-albedo process active.

Figure 7

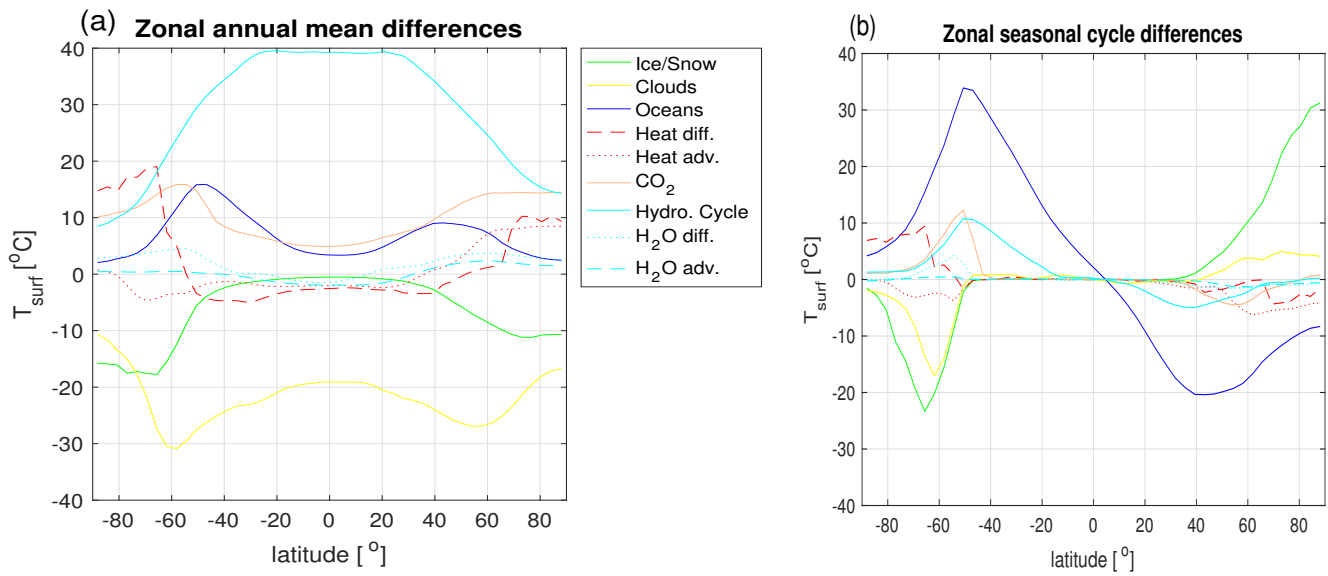


Figure 7: Zonal mean values of the annual mean (a) and seasonal cycle differences (b) for the experiments as shown in Figs. 5 and 6. g) The mean for the hydrological cycle is for the experiments with and without the ice-albedo process active.

Figure 8 part 1

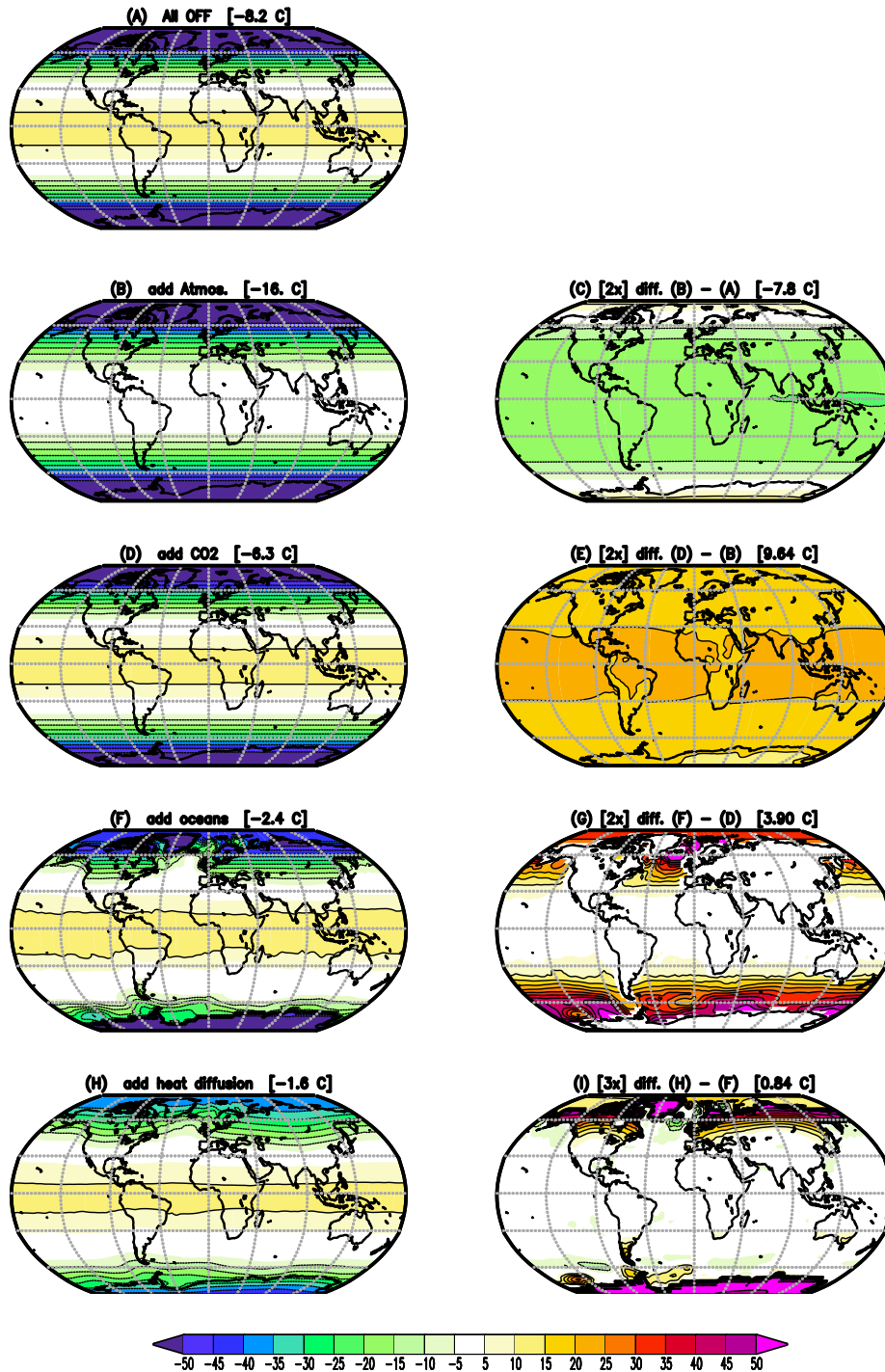


Figure 8: Conceptual build-up of the annual mean climate: starting with all processes turned OFF (a) and then adding more processes in each row: (b) atmosphere, (d) CO₂, (f) oceans, (h) heat diffusion, (j) heat advection, (l) ice-albedo, (n) hydrological cycle, (p) clouds and (r) water vapour transport. The panels on the right column show the difference of the left panel to the previous row left panel. Global mean values are shown in the heading. All values are in oC. In some panels in the right column the values are scaled for better comparison: (e), (g) and (q) by a factor of 2, (i) and (m) by a factor of 3 and (c), (k) and (s) by a factor of 4. For details see on the experiments see section 2a.

Figure 8 part 2

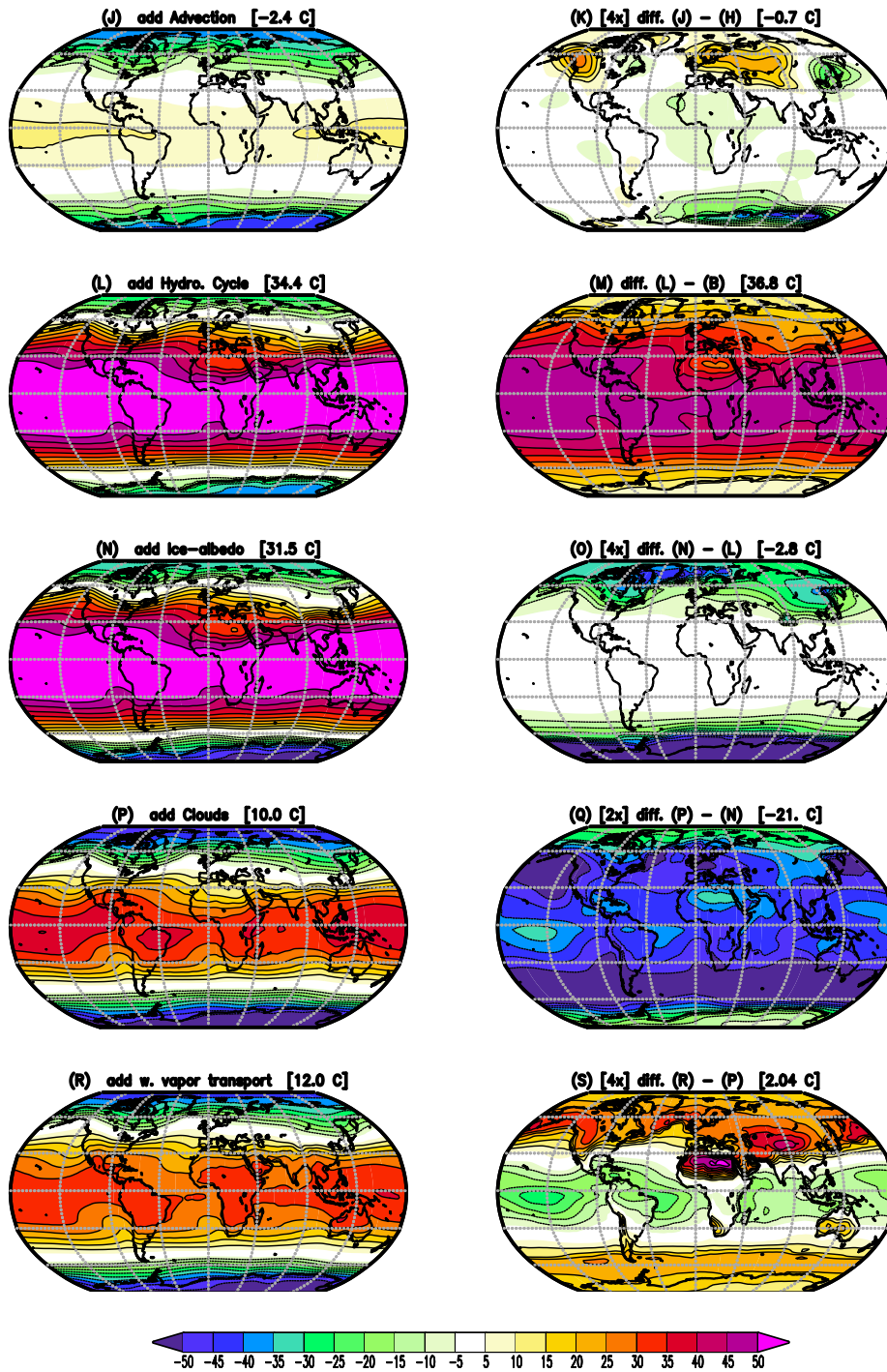


Figure 9 part 1

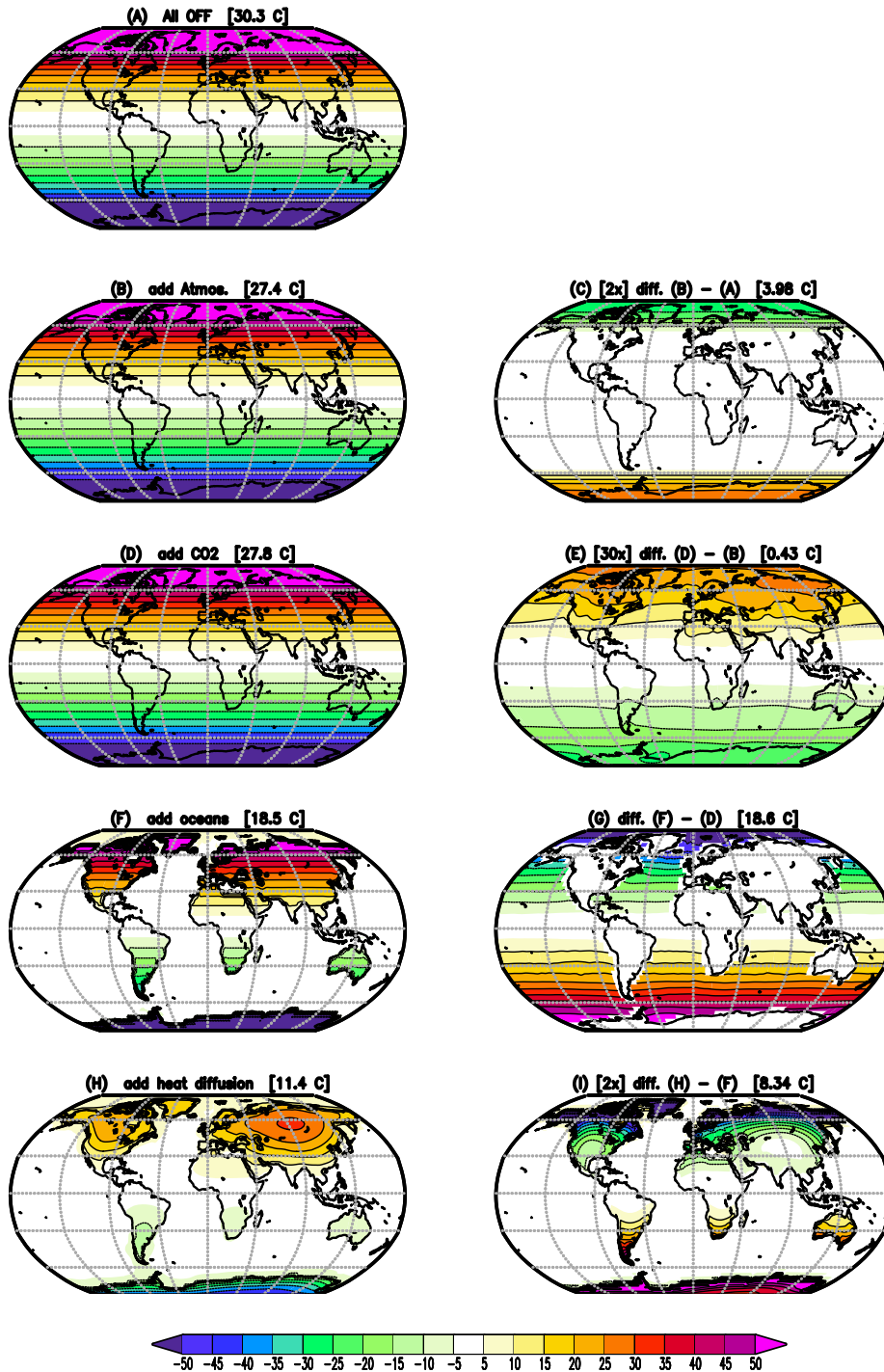


Figure 9: As in Fig. 8, but conceptual build-up of the seasonal cycle. The seasonal cycle is defined by the difference between the month [JAS] - [JFM] divided by two. Global mean absolute values are shown in the heading. In some panels in the right column the values are scaled for better comparison: (c) and (o) by a factor of 2, (i), (k), (q) and (s) by a factor of 5 and for (e) by a factor of 30.

Figure 9 part 2

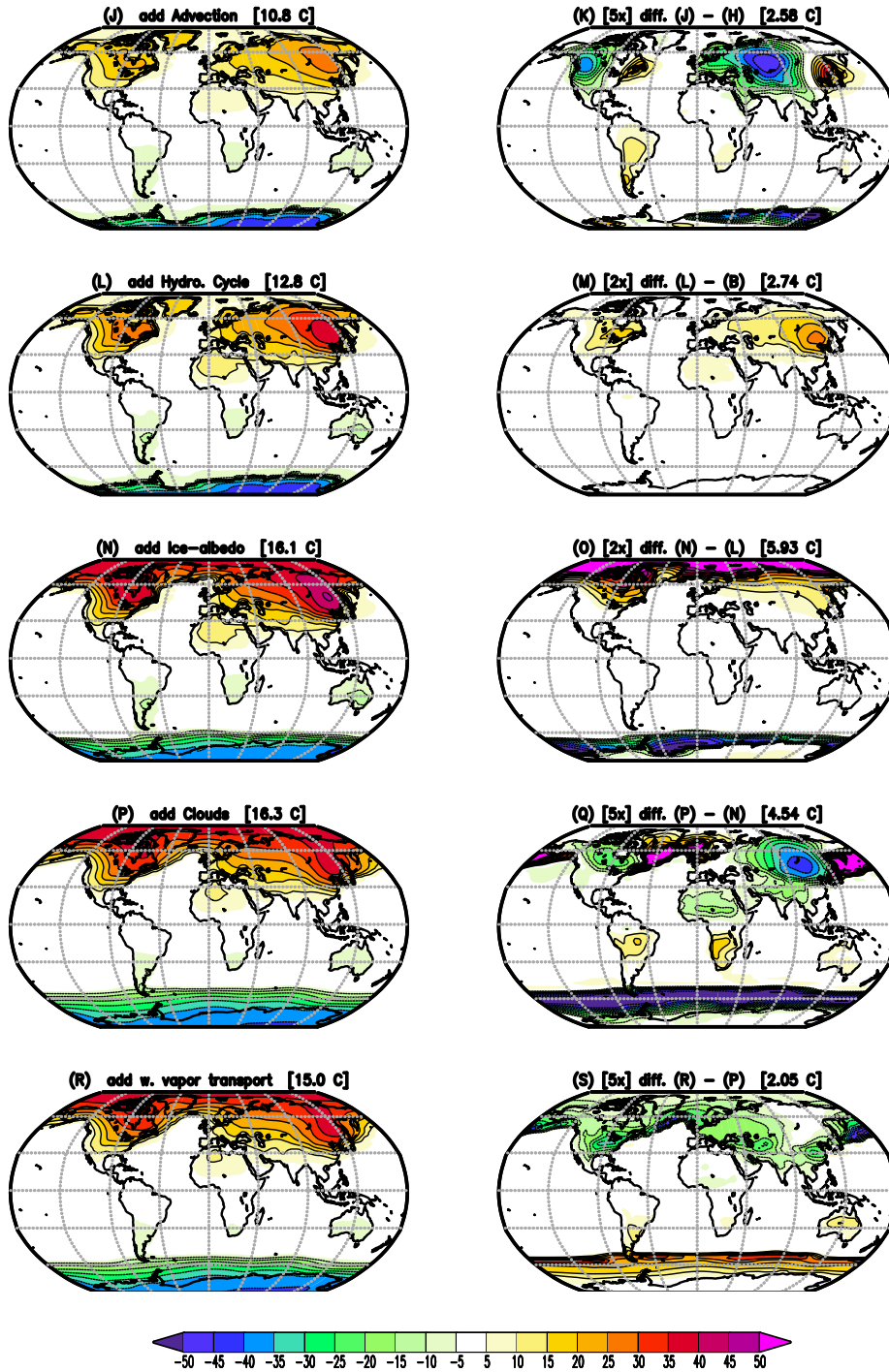


Figure10

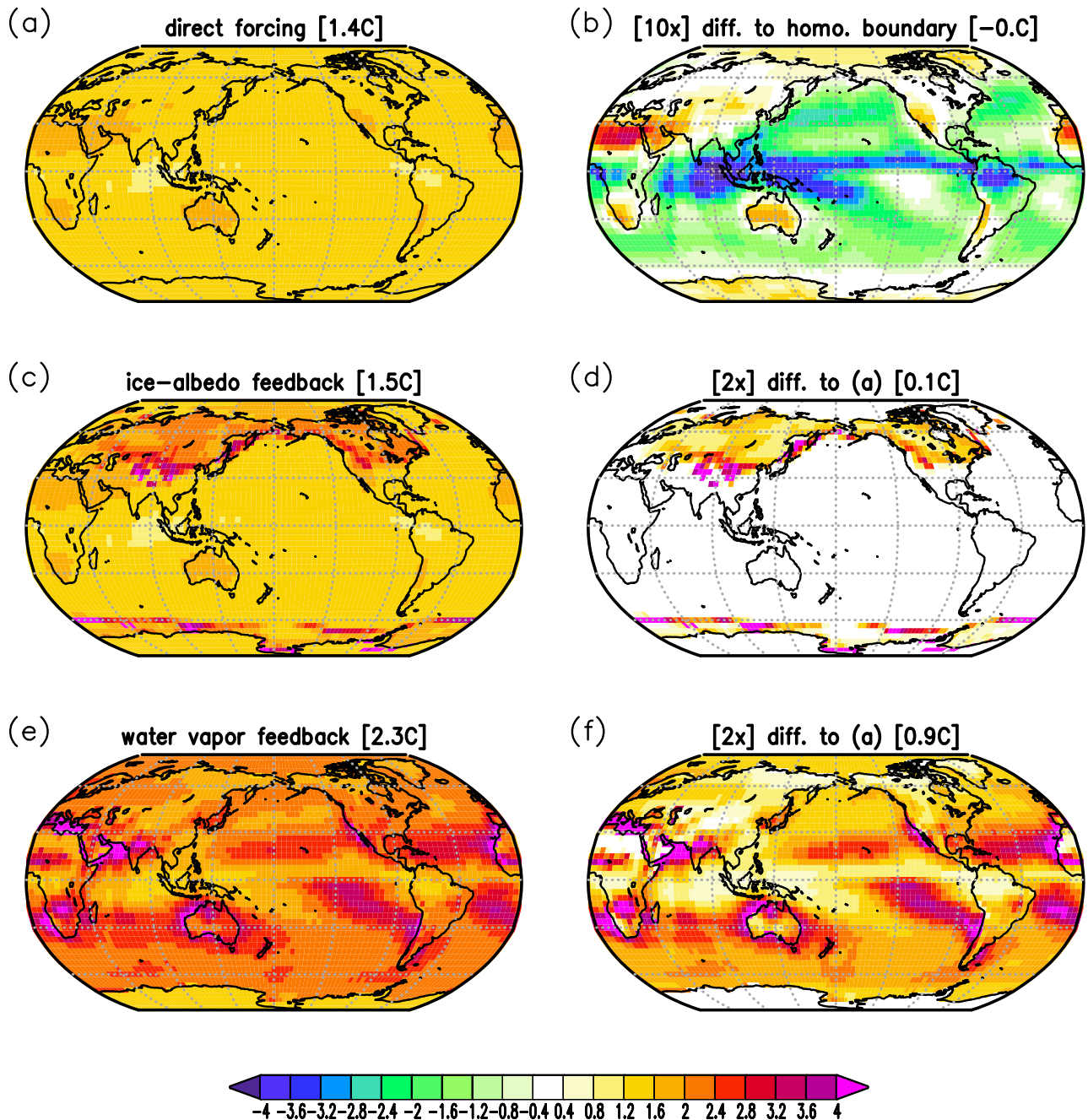


Figure 10: Local T_{surf} response to doubling of the CO_2 concentration in experiments without atmospheric transport (each point on the maps is independent of the others). (a) GREB with topography, humidity and cloud processes and all other processes OFF. (b) difference of (a) to GREB with topography and all other processes OFF scaled by a factor of 10. (c) GREB model as in (a), but with ice-albedo process ON. (d) difference of (c)-(a) scaled by a factor of 2. (e) GREB model as in (a), but with hydrological cycle process ON. (f) difference of (e)-(a) scaled by a factor of 2. For details see on the experiments see section 2b.

Figure 11

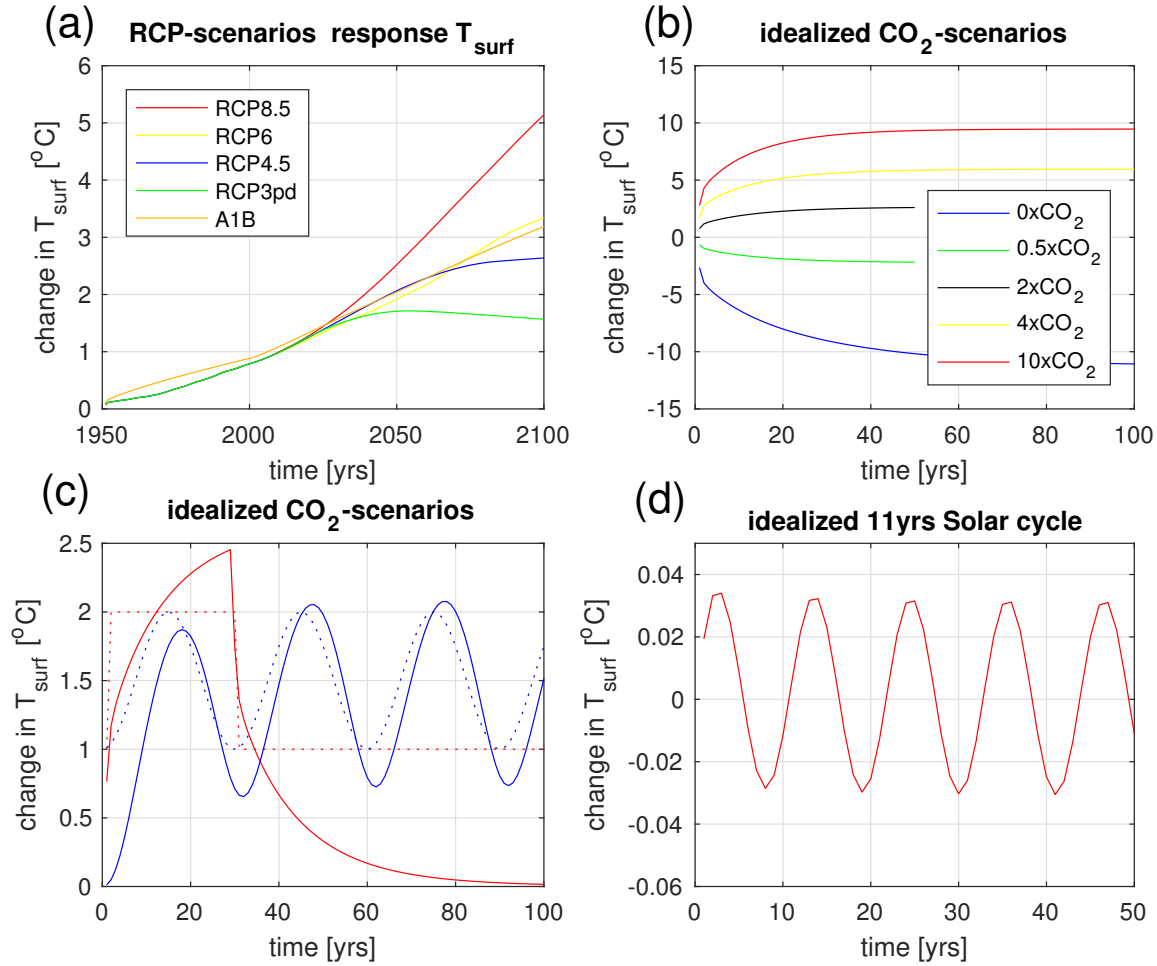


Figure 11: Global mean T_{surf} response to idealized forcing scenarios: (a) different RCP CO_2 forcing scenarios. (b) Scaled CO_2 concentrations. (c) idealized CO_2 concentration time evolutions (dotted lines) and the respective T_{surf} responses (solid lines of the same colour) for the 2x CO_2 abrupt reverse (red) and the 2x CO_2 wave (blue) simulations. (d) idealized 11yrs solar cycle. List of experiments is given in Table 3.

Figure 12

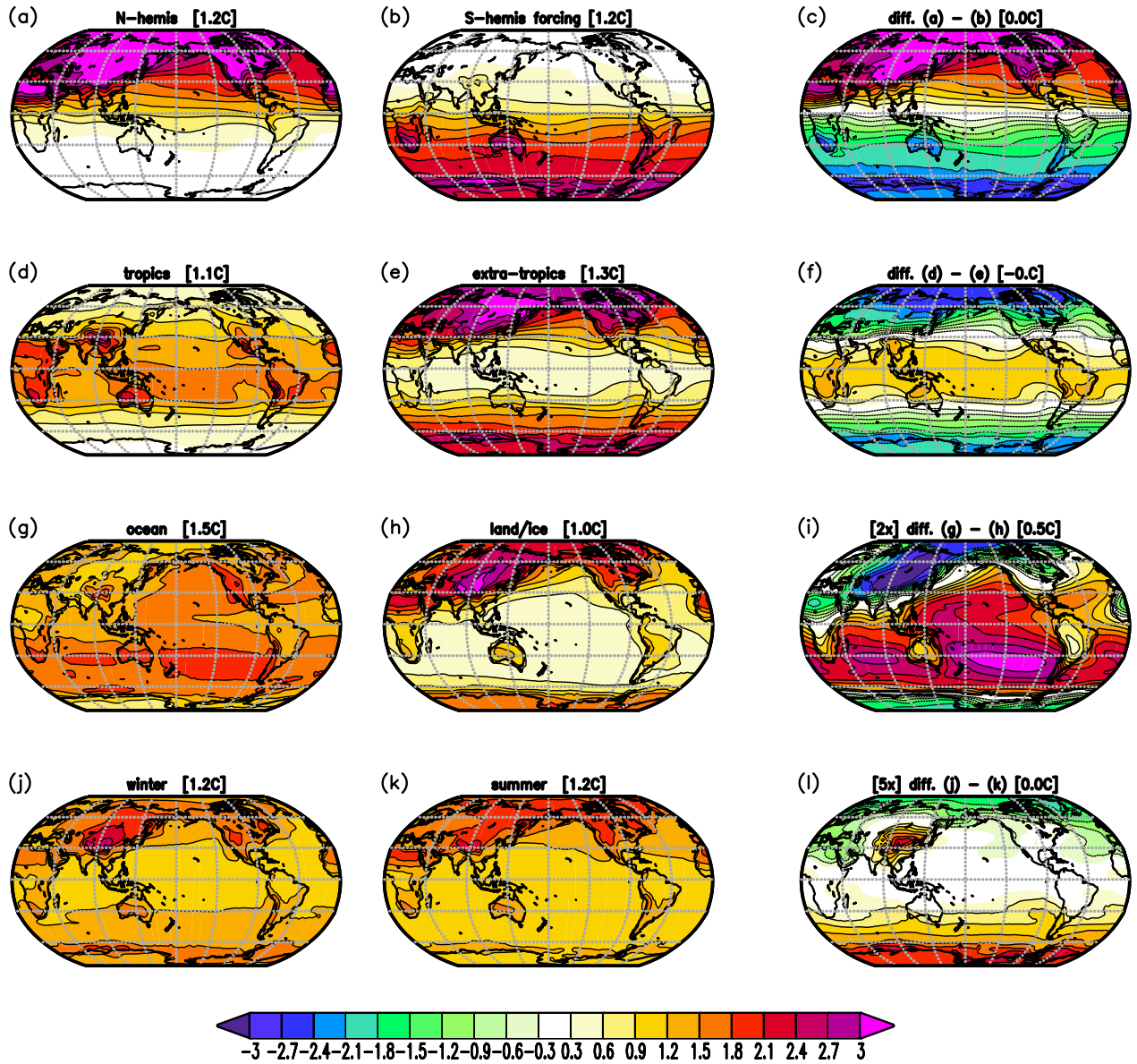


Figure 12: T_{surf} response to partial doubling of the CO_2 concentration in: Northern (a) and Southern (b) hemisphere, tropics (d) and extra-tropics (e), oceans (g) and land (h), and in boreal winter (j) and summer (k). The right column panels show the difference between the two panels two the left in the same row.

Figure 13

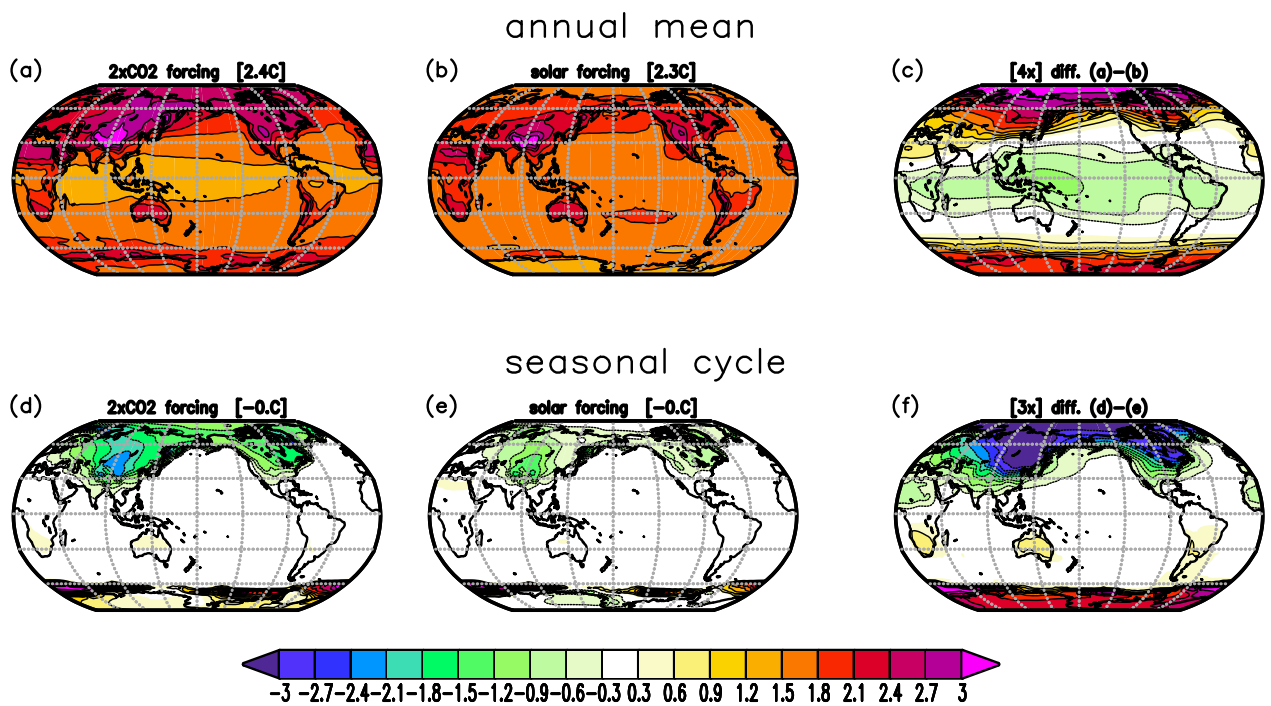


Figure 13: T_{surf} response to changes in the solar constant by $+27W/m^2$ (middle column) versus a doubling of the CO_2 concentration (left column) for the annual mean (upper) and the seasonal cycle (lower). The seasonal cycle is defined by the difference between the month [JAS] - [JFM] divided by two. The right column panels show the difference between the two panels two the left in the same row scaled by 4 (c) and 3 (f).

Figure 14

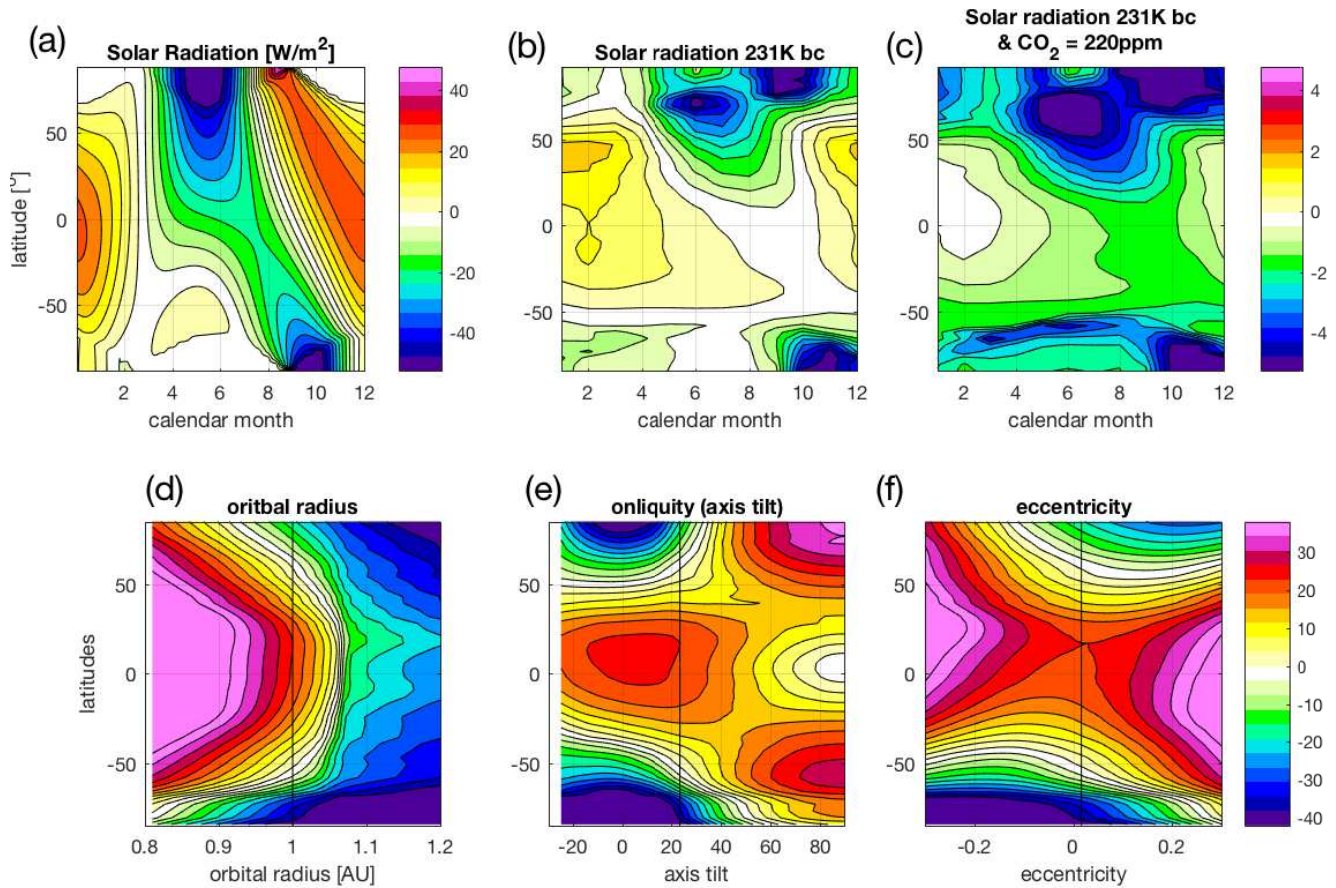


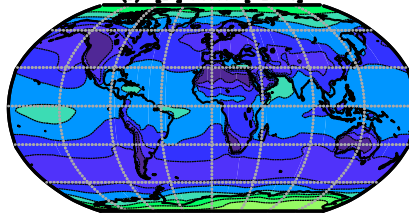
Figure 14: Orbital parameter forcings and T_{surf} responses: (a) incoming solar radiation changes in the Solar-231Kyr experiment relative to the control GREB model. T_{surf} response in Solar-231Kyr (b) and Solar-231Kyr-200ppm (c) relative to the control GREB model. Annual mean T_{surf} in Orbit-radius (d), Obliquity (e) and Eccentricity (f). The solid vertical line in (d)-(f) marks the control (today) GREB model.

Supplementary Figure 1

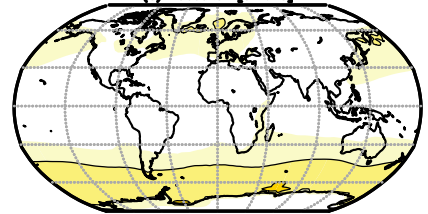
(A) [3x] Ice/Snow [0 C]

Entire Grid Undefined

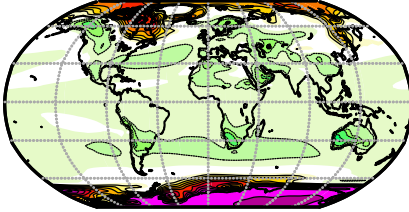
(B) [2x] clouds [-20. C]



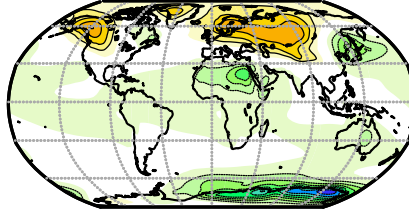
(C) Oceans [5.16 C]



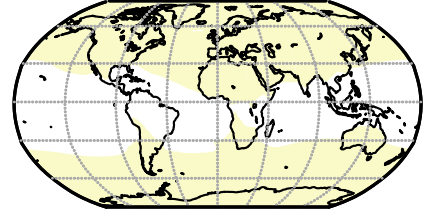
(D) [3x] heat diffusion [-0.8 C]



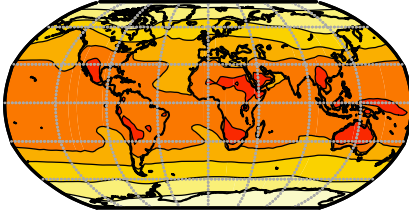
(E) [3x] heat advection [-1.4 C]



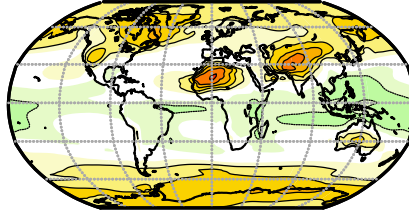
(F) CO2 [5.85 C]



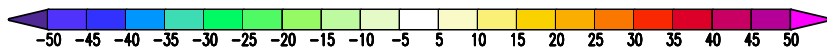
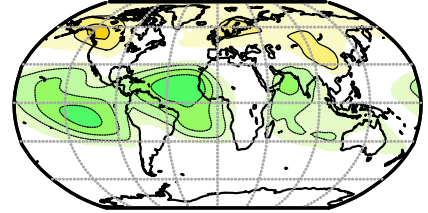
(G) Hydrological cycle [23.2 C]



(H) [6x] water vapor diffusion [0.47 C]



(I) [6x] water vapor advection [-0.2 C]



Supplementary Figure 2

